90_23

Optimal Control of the Penicillin G Fed–Batch Fermentation : An Analysis of the Model of Heijnen et al.

Jan F. Van Impe
Department of Electrical Engineering
Katholieke Universiteit Leuven
Kardinaal Mercierlaan 94 B-3001 Leuven Belgium
tel: 32/16/220931 fax: 32/16/221855
email: vanimpe@esat.kuleuven.ac.be

Bart M. Nicolaï
Department of Agricultural Engineering
Katholieke Universiteit Leuven
Kardinaal Mercierlaan 92 B-3001 Leuven Belgium
tel: 32/16/220931 fax: 32/16/205032

Peter A. Vanrolleghem
Department of Agricultural Engineering
Rijksuniversiteit Gent
Coupure Links 653 B-9000 Gent Belgium
tel: 32/91/236961 fax: 32/91/330354

Jan A. Spriet
Department of Agricultural Engineering
Katholieke Universiteit Leuven

Bart De Moor and Joos Vandewalle
Department of Electrical Engineering
Katholieke Universiteit Leuven

ESAT–SISTA Report 1990–23

August 1, 1990

90-23

Van Impe J., Nicolaï B., Vanrolleghem P., Spriet J., De Moor B., Vandewalle J., ``Optimal control of the penicillin G fed-batch fermentation: an analysis of the model of Heijnen et al", *Optimal control applications & methods*, vol. 15, no. 1, 1994, pp. 13-34., Lirias number: 73187.

Abstract

Optimal Control of the Penicillin G Fed-Batch Fermentation : An Analysis of the Model of Heijnen et al.

Summary

This paper presents the application of Optimal Control theory in determining the optimal feed rate profile for the penicillin G fed–batch fermentation, using a mathematical model based on balancing methods. As this model does not fulfil all requisites for standard Optimal Control, we propose a sequence of new models—that converges to the original one in a smooth way—to which the standard techniques are applicable, and develop an efficient computational algorithm. The unusual optimization of some initial conditions is included. We state then the conjecture that allows to obtain the Optimal Control for the original model. Mathematical and microbial insight leads to the construction of a suboptimal heuristic strategy—which we show to be a limiting case of the optimal scheme—that can serve as a basis for the development of more practical and reliable control schemes.

Key Words Optimal Control, Non–linear systems, Penicillin Fed–Batch Fermentation, Biotechnological Modeling

1 Introduction

Nowadays penicillin G is an almost common antibiotic; nevertheless the fermentation technology and the mathematical description of the production process are still a subject of interest. Compared with conventional chemical industries, the fermentation industry is quite reluctant to use advanced control and optimization methods. Some plausible reasons are the lack of adequate dynamic models suitable for control purposes, the lack of on–line sensors for substrates, biomass and products, the communication problem between microbiologists, biochemists and control engineers by lack of a common language,...

In recent years there has been a growing interest in the modeling of penicillin fermentation processes. There are at least two unstructured fed–batch models available in the literature that pretend to describe the penicillin G fermentation in a more or less correct way : the model of Heijnen, Roels and Stouthamer[1] and the one of Bajpai and Reuß[2]. In optimizing the substrate feed rate a lot of work has been done on the second model[3–6]. Starting from their structural differences, we shall give a detailed comparison of these models from the control engineering viewpoint in another paper[7].

In this paper we present for the first time the application of Optimal Control theory to the model of Heijnen et al.[1], in verifying the authors' statement that *the glucose feed scheme is of crucial importance in obtaining high penicillin yields.* As this model does not fulfil all requisites for standard Optimal Control, we propose a sequence of new models—that converges to the original one in a smooth way—to which the standard techniques are applicable.

The paper is organized as follows : Section 2 presents the original model of Heijnen et al. and the modifications to make it suitable for standard Optimal Control, with the statement of the complete optimization problem. We also formulate the basic conjecture of this paper. Section 3 describes the optimal feed rate profile that maximizes the final amount of product. In Section 4 we derive a suboptimal strategy based on the mathematical and microbial knowledge, that is found to be a useful alternative for the optimal open–loop feed rate profile and opens perspectives for more reliable model–independent control schemes. Some conclusions are formulated in Section 5. Some theoretical results are presented in the Appendices.

2 The model of Heijnen, Roels and Stouthamer and the necessary modifications for Optimal Control

Let us first introduce some notations to be used throughout this paper :

t	: time (hr)
S	: amount of substrate in broth (mol) (Glucose)
X	: amount of cell mass in broth (mol DM)
P	: amount of product in broth (mol) (Penicillin)
G	: total broth weight (kg)

u	: input substrate feed rate (mol/hr)
C_s	: $\triangleq S/G$ substrate concentration in broth (mol/kg)
C_x	: $\triangleq X/G$ cell mass concentration in broth (mol DM/kg)
C_p	: $\triangleq P/G$ product concentration in broth (mol/kg)
s_F	: feed substrate concentration (mol/kg)
α	: total amount of substrate available for fermentation (mol)
σ	: specific substrate consumption rate (mol/mol DM hr)
μ	: specific growth rate (hr^{-1})
μ_{crit}	: critical specific growth rate (hr^{-1})
B	: Dabes constant (hr^{-1})
π	: specific production rate (mol/mol DM hr)
r_c	: net rate of CO_2 conversion (mol/hr)
r_n	: net rate of nitrogen source conversion (mol/hr)
r_o	: net rate of oxygen conversion (mol/hr)
r_{su}	: net rate of sulphate source conversion (mol/hr)
$Q_{s,max}$	: maximum specific sugar uptake rate (mol/mol DM hr)
$Q_{p,max}$	: maximum specific penicillin synthesis rate (mol/mol DM hr)
K_s	: Michaelis constant for sugar uptake (mol/kg)
m_s	: maintenance constant (mol/mol DM hr)
k_h	: penicillin hydrolysis or degradation constant (hr^{-1})
$Y_{x/s}$	: cell mass on substrate yield (mol DM/mol)
$Y_{p/s}$	: product on substrate yield (mol/mol)

2.1 The original model of Heijnen et al.

Heijnen et al.[1] used the following steps in the construction of a simple unstructured model for a fermentation process with product formation (e. g. penicillin G) : definition of relevant compounds in the penicillin fermentation, formulation of elemental balances and the enthalpy balance—one of the most interesting features of this approach—, formulation of mass–balances and the weight–balance, selection of the kinetic equations—in this case based on a literature survey—. Their research resulted in the following continuous–time model which they believe to be of great possible help in the optimization of the process :

$$\frac{dS}{dt} = -\sigma X + u \tag{1}$$

$$\frac{dX}{dt} = \mu X \tag{2}$$

$$\frac{dP}{dt} = \pi X - k_h P \tag{3}$$

$$\frac{dG}{dt} = \frac{1}{s_F} u - 0.0008G - 0.044 r_c + 0.068 r_n + 0.392 r_{su} + 0.032 r_o + 0.68 \pi X \tag{4}$$

In the last equation, terms with a positive sign are due to the input of respectively glucose, nitrogen source, sulphate source, oxygen and precursor. Terms with a negative sign represent respectively evaporation and carbon dioxide production. For more details see Reference 1.

The specific substrate consumption rate is given by a *Monod*-type[8] relationship :

$$\sigma = Q_{s,max}\frac{C_s}{K_s + C_s} \tag{5}$$

Hydrolysis of penicillin to penicilloic acid is modeled by a first-order reaction. The specific production rate is assumed to be growth-coupled, and is modeled by a *Blackman*-type[8] relationship—note that the original Blackman-kinetics specified μ as a function of C_s— :

$$\pi(\mu) = Q_{p,max}\begin{cases} \mu/\mu_{crit} & \text{for } \mu \leq \mu_{crit} \\ 1 & \text{for } \mu \geq \mu_{crit} \end{cases} \tag{6}$$

As a consequence of balancing, the specific growth rate is then defined by :

$$\mu = Y_{x/s}(\sigma - m_s - \pi/Y_{p/s}) \tag{7}$$

which represents an *endogenous* metabolism.

Table 1 shows the parameters and initial conditions—denoted with a subscript "$_0$"—we have used in all simulations. The expressions for the rates r_c, r_n, r_o and r_{su} can be found back in Reference 1.

parameters			
Q_s, max	0.0245	Q_p, max	$3.3\ 10^{-4}$
K_s	0.0056	μ_{crit}	0.01
$Y_{x/s}$	3.67	k_h	0.002
$Y_{p/s}$	0.46	s_F	1/0.36
m_s	0.0034		
initial conditions			
X_0	4000	S_0	*to be specified*
P_0	0	G_0	$98020 + S_0/s_F$
t_0	0	α	205500

Table 1 *Parameters and initial conditions used in simulations*

2.2 Statement of the optimization problem

Let us now turn our attention to the structure of f. Equation (5) tells us that σ is a function of C_s only. Substitution of equations (5) and (6) in equation (7) delivers an implicit relationship between μ and C_s, the solution for μ of which could be used in equation (6). We conclude that the three specific rates σ, μ and π are functions of C_s *only*. Figure 1 shows the result of these manipulations. As π has a discontinuity in the derivative with respect to μ for $\mu = \mu_{crit}$, it is quite clear that π as a function of C_s exhibits a corner at the corresponding value of C_s, say $C_{s,crit}$.

Figure 1a *The specific rates σ and μ as functions of C_s*
Figure 1b *The specific rate π as a function of C_s*

Remark that in the right-hand side of equation (4) all terms except the first one—representing the input of glucose—have negligible influence on the dynamics and final value of the most interesting variable $P_f \triangleq P(t_f)$. All simulations were carried out using the routines *D02EBF* and *D02EHF* from the *NAG-Library* on a *VAX-VMS* machine. For instance, for $S_0 = 5500$ mol and a constant input $u = 1000$ mol/hr during 200 hours, one obtains $P_f = 3001.12$ mol using the complete equation for G, and a value which is only 0.03% smaller when using only the first term.

This can be seen as follows. As the specific rate π is a function of C_s only, the time evolution of P can be calculated from equation (3), if we have a differential equation for C_s :

$$\frac{dC_s}{dt} = \frac{1}{G}\frac{dS}{dt} - \frac{C_s}{G}\frac{dG}{dt} \tag{8}$$

For π out of saturation, typical orders of magnitude are : $C_s = O(10^{-3})$, $\mu = O(10^{-3})$, $\pi = O(10^{-4})$. Using the exact expressions for the specific rates r_c, r_n, r_o and r_{su} (Reference 1) in the right-hand side of equation (4), it can be seen that under these conditions, the second most important contribution comes from the term representing evaporation. So the above equation can be written as follows :

$$\frac{dC_s}{dt} = -\sigma C_x + (1 - \frac{C_s}{s_F})\frac{u}{G} + 0.0008C_s + \text{l.o.t.} \tag{9}$$

With u in the order of magnitude of 1000 mol/hr, it is clear that the term $0.0008C_s$ has a negligible influence on the dynamics of C_s.

So in optimizing the glucose feeding policy, we *neglect* all these terms to simplify the analytical development and our model reduces to :

$$\frac{dS}{dt} = -\sigma X + u \tag{10}$$

$$\frac{dX}{dt} = \mu X \tag{11}$$

$$\frac{dP}{dt} = \pi X - k_h P \tag{12}$$

$$\frac{dG}{dt} = \frac{1}{s_F}u \tag{13}$$

Another advantage is that we can take care of an isoperimetric constraint on the input *without* introducing an extra equation, as we shall see further on.

An obvious choice for a state space vector is given by :

$$\mathrm{x} = \begin{pmatrix} x_1 \\ x_2 \\ x_3 \\ x_4 \end{pmatrix} \triangleq \begin{pmatrix} S \\ X \\ P \\ G \end{pmatrix} \tag{14}$$

and with the definition of :

$$\mathbf{f} = \begin{pmatrix} f_1 \\ f_2 \\ f_3 \\ f_4 \end{pmatrix} \triangleq \begin{pmatrix} -\sigma X \\ \mu X \\ \pi X - k_h P \\ 0 \end{pmatrix} \qquad \mathbf{b} = \begin{pmatrix} b_1 \\ b_2 \\ b_3 \\ b_4 \end{pmatrix} \triangleq \begin{pmatrix} 1 \\ 0 \\ 0 \\ 1/s_F \end{pmatrix} \tag{15}$$

we obtain the following state space model linear in the control u :

$$\frac{d\mathbf{x}}{dt} = \mathbf{f}(\mathbf{x}) + \mathbf{b}u \tag{16}$$

Remark that, due to equation (7) :

$$f_2 = Y_{x/s}(-f_1 - m_s X - (f_3 + k_h P)/Y_{p/s}) \tag{17}$$

Numerical values for the initial conditions are mentioned in Table 1. $x_{2,0}$ and $x_{3,0}$ are given, $x_{1,0}$ and $x_{4,0}$ are related by :

$$x_{4,0} = G_* + x_{1,0}/s_F \tag{18}$$

where G_* denotes the given initial weight *without* substrate.

The optimization problem we consider in this paper is to determine for the given set of differential equations (10)–(13) the optimal feed rate profile that minimizes the performance index :

$$J(u) = g(\mathbf{x}(t_f)) \triangleq -P(t_f) \tag{19}$$

i. e. maximizes the final amount of product, subject to the following constraints :

- $t_0 = 0$, $t_f =$ free
- all variables have to be kept positive, i. e. for all t in $[0, t_f]$:

$$x_i(t) \geq 0, \text{ for } i = 1, \ldots, 4 \qquad u(t) \geq 0 \tag{20}$$

- the initial amount of substrate $x_{1,0}$ is *free*; the initial conditions $x_{1,0}$ and $x_{4,0}$ are only constrained by equation (18). In other words, some initial conditions can be manipulated to minimize the performance measure, so (19) should be replaced by :

$$J \equiv J(u, \mathbf{x}_0) = g(\mathbf{x}(t_f)) = -x_3(t_f) \tag{21}$$

- the total amount of feed is fixed, i. e. :

$$x_{1,0} + \int_{t_0}^{t_f} u(t)\, dt = \alpha \tag{22}$$

Notice that the last *isoperimetric* constraint on the input is equivalent to a *physical* constraint of the form — due to differential equation (13) — :

$$x_{4,f} \equiv G(t_f) = G_f, \; G_f \text{ fixed} \tag{23}$$

2.3 A modified model and the basic conjecture

As mentioned above, some partial derivatives $\partial f_i/\partial x_j$ are not continuous. So we cannot apply standard Optimal Control theory—see e. g. Reference 9. To circumvent this problem, we shall replace the piecewise-smooth Blackman-kinetics $\pi(\mu)$ by a family of completely smooth curves that converge as a function of one parameter to the original kinetics.

Consider the following relationship between μ and π, the *Dabes-kinetics*[8] with A and B parameters—note that the original Dabes-kinetics specified C_s as a function of μ— :

$$\mu = A\pi + \frac{B\pi}{Q_{p,max} - \pi} \tag{24}$$

or, in another way :

$$A\pi^2 - (Q_{p,max}A + B + \mu)\pi + Q_{p,max}\mu = 0 \tag{25}$$

Solving this quadratic equation for π and taking the negative sign—as for $\mu = 0$ we want $\pi = 0$ as in the Blackman-kinetics—leads to :

$$\pi(\mu) = \frac{(Q_{p,max}A + B + \mu) - \sqrt{(Q_{p,max}A + B + \mu)^2 - 4AQ_{p,max}\mu}}{2A} \tag{26}$$

We now eliminate one parameter, say A, by solving :

$$\frac{d\pi}{d\mu}(\mu = 0) = \frac{Q_{p,max}}{\mu_{crit}} \tag{27}$$

which imposes that the derivative of π for $\mu = 0$ must be equal to the value given in equation (6). The solution is :

$$A = \frac{\mu_{crit} - B}{Q_{p,max}} \tag{28}$$

and thus we obtain :

$$\pi(\mu) = Q_{p,max}\frac{(\mu + \mu_{crit}) - \sqrt{(\mu + \mu_{crit})^2 - 4(\mu_{crit} - B)\mu}}{2(\mu_{crit} - B)} \tag{29}$$

which is the desired family of smooth curves, where B is the only parameter that must lie between $0 < B < \mu_{crit}$.

Let us consider now the boundaries for the parameter B. For $B \to \mu_{crit}$, A tends to 0, and the above equation becomes undetermined. However, solving the original Dabes-kinetics (24) for π with $A = 0$ delivers the following *Monod*-type law :

$$\pi(\mu) = Q_{p,max}\frac{\mu}{\mu_{crit} + \mu} \tag{30}$$

which is of course also a completely smooth relationship.

On the other hand, as $B \rightarrow 0$ we obtain readily :

$$\pi(\mu) = Q_{p,max}\frac{(\mu + \mu_{crit}) - \sqrt{(\mu - \mu_{crit})^2}}{2\mu_{crit}} = \frac{Q_{p,max}}{2\mu_{crit}}(\mu + \mu_{crit} - \mid \mu - \mu_{crit} \mid) \qquad (31)$$

which is in fact another form of the *Blackman* law (6).

So we can refine the boundaries for B to $0 < B \leq \mu_{crit}$. We conclude that we have constructed a one-dimensional family of curves—and thus a family of models—that are completely smooth within the given boundaries of the parameter B, thus assuring the continuity of $\partial f_i/\partial x_j$ for all i and j. Moreover, as $B \stackrel{>}{\rightarrow} 0$, we come arbitrarily close to the original model. In Figure 2 we show some members of this family for different values of B.

Figure 2 *Dabes-kinetics $\pi(\mu)$ for some values of parameter B*

Obviously, we can determine the optimal control $u(B,t)$ for every B within the given boundaries, using standard optimal control theory. For the original model—corresponding to $B = 0$—we shall have to calculate the optimal control in another way. The following conjecture indicates how we can do that.

Conjecture 1 *Suppose that we have a convergent sequence of models $\mathcal{M}(\mathrm{p})$ — p denotes a set of parameters — i. e. :*

$$lim_{\mathrm{p}\rightarrow\mathrm{p_0}}\mathcal{M}(\mathrm{p}) \stackrel{\triangle}{=} \mathcal{M}_0$$

Suppose that for every model $\mathcal{M}(\mathrm{p})$, with $\mathrm{p} \neq \mathrm{p_0}$, we can determine the optimal control $u(\mathrm{p},t)$ that minimizes some cost index $J(u)$ with standard optimal control theory.
Then the sequence of optimal controls $u(\mathrm{p},t)$ is convergent, i. e. :

$$lim_{\mathrm{p}\rightarrow\mathrm{p_0}}u(\mathrm{p},t) \stackrel{\triangle}{=} u_0(t)$$

Moreover, this limit $u_0(t)$ is the optimal control for model $\mathcal{M}_0$ minimizing $J(u)$.

This conjecture seems somewhat trivial if we can obtain the optimal control for the limit model in a *direct* way. However, it provides a useful methodology in calculating optimal controls for models to which standard techniques are *not* applicable.

As we shall see further on, setting $B = 10^{-10}$ in equation (29) is a very accurate approximation in simulating the original Blackman-kinetics (6). The results of a simulation with a constant feed rate profile are shown in Figure 3. With $S_0 = 5500$ mol and $t_f = 200$ hr, $u(t) = 1000$ mol/hr according to constraint (22). The final amount of penicillin is $P(t_f) = 3001.1$ mol.

Figure 3 *Constant glucose feed rate and corresponding cell, glucose, product, μ and π profiles*

Some comments are in order here. As Heijnen et al. remarked, the simulation results for $S(t)$, $X(t)$ and $P(t)$ are obviously in agreement with the classification of the penicillin fermentation in the group of product formation processes of the non–growth–associated type . In agreement with the experimentally observed behaviour, the penicillin fermentation process behaves as a *biphasic* process : a *growth*–phase *(tropophase)* of rapid cell growth and almost no production, followed by a *production*–phase *(idiophase)* with almost no growth. However, Heijnen et al. obtained this separation in their model on the assumption of a *direct* coupling between specific production rate and specific growth rate—equation (6)! The μ and π profiles in Figure 3 illustrate some of these ideas. Heijnen et al. conclude that the biphasic behaviour of the penicillin fermentation does not necessarily mean that penicillin is of the non–growth–associated type, as with their model they can describe most of the phenomena observed in practice. It may be clear that this discussion belongs to the field of microbiologists and biochemists. However, from the mathematical point of view, the commonly observed separation between growth and production phase is a quite useful feature in optimizing the process.

3 Optimal Control of the modified model

In this section, we derive the optimal control $u(B,t)$ for the given optimization problem. The methodology developed below can be used for every B in $0 < B \leq \mu_{crit}$. However, as indicated in the previous section, we are especially interested in the optimal control for B approximating zero. The uncommon optimization of some initial conditions of the state shall be included.

3.1 Statement of the control problem

The Hamiltonian H for this problem is given by

$$H = \lambda^{\mathrm{T}}(\mathrm{f}(\mathrm{x}) + \mathrm{b}u) \triangleq \phi + \psi u \tag{32}$$

where λ is the 4×1 vector of *adjoint* variables. The superscript "T" denotes the transpose of a vector. The scalar functions ϕ and ψ are given by :

$$\phi = \lambda_1 f_1 + \lambda_2 f_2 + \lambda_3 f_3 \qquad\qquad \psi = \lambda_1 + \lambda_4 / s_F \tag{33}$$

The adjoint vector λ satisfies the following system of differential equations :

$$\frac{d\lambda}{dt} = -\frac{\partial H}{\partial \mathrm{x}} = -\frac{\partial \mathrm{f}}{\partial \mathrm{x}}^{\mathrm{T}} \lambda \tag{34}$$

or

$$\begin{pmatrix} \dot{\lambda}_1 \\ \dot{\lambda}_2 \\ \dot{\lambda}_3 \\ \dot{\lambda}_4 \end{pmatrix} = \begin{pmatrix} -\partial f_1/\partial x_1 & -\partial f_2/\partial x_1 & -\partial f_3/\partial x_1 & 0 \\ \sigma & -\mu & -\pi & 0 \\ 0 & 0 & k_h & 0 \\ -\partial f_1/\partial x_4 & -\partial f_2/\partial x_4 & -\partial f_3/\partial x_4 & 0 \end{pmatrix} \begin{pmatrix} \lambda_1 \\ \lambda_2 \\ \lambda_3 \\ \lambda_4 \end{pmatrix} \tag{35}$$

Note that in order to compute $\partial f_i/\partial x_1$ and $\partial f_i/\partial x_4$, $i = 2, 3$, we need $\partial\mu/\partial x_1$ and $\partial\mu/\partial x_4$, which can be calculated by substituting equation (29) in equation (7) and taking the *implicit* derivatives with respect to x_1 and x_4.

Together with the state equations (16), we obtain a system of $2 \times n$ first order differential equations—where n denotes the dimension of the state vector x—which requires the specification of $2 \times n$ boundary conditions.

These can be specified as follows :

- $x_{2,0}$ and $x_{3,0}$ are given
- $x_{1,0}$ and $x_{4,0}$ are interrelated by equation (18)
- $x_{4,f}$ is given due to equation (23)
- $\lambda_{i,f}$, $i = 1, \ldots, 3$ are given by — with g specified in (21) — :

$$\lambda_{i,f} = \frac{\partial g}{\partial x_i}(t_f)\,. \tag{36}$$

which gives :

$$\begin{pmatrix} \lambda_{1,f} \\ \lambda_{2,f} \\ \lambda_{3,f} \end{pmatrix} = \begin{pmatrix} 0 \\ 0 \\ -1 \end{pmatrix} \tag{37}$$

It should be clear that we need still another boundary condition, as $x_{1,0}$ and $x_{4,0}$ are not given explicitly. It can be shown (see Appendix 1) that the missing condition is given by :

$$\psi(0) \equiv \lambda_{1,0} + \lambda_{4,0}/s_F = 0 \tag{38}$$

We call a control $u(t)$ *admissible* if it satisfies all the constraints of the problem. All conditions being necessary conditions, we can only obtain *extremal* solutions $(\mathrm{x}^*, \lambda^*, u^*)$ which must be checked for optimality. An extremal control $u^*(t)$ follows from the minimization of the Hamiltonian H over all admissible control functions :

$$\min_{\text{all admiss } u} H(\mathrm{x}^*, \lambda^*, u) = H(\mathrm{x}^*, \lambda^*, u^*) \tag{39}$$

which is Pontryagin's Minimum Principle[10] for this case.

Remark that the Optimal Control approach gives rise to a *two point boundary value problem (TPBVP)*.

Since the state equations (16) and the cost index (21) are time–invariant, the Hamiltonian H remains constant along an optimal trajectory. As the final time t_f is free, we know that $H = 0$.

3.2 Optimal Control with bounded input and fixed initial state

As a first step in the solution, we shall solve the given problem subject to an *additional* constraint on the input, and with the *complete* initial state being given. So suppose $x_{1,0}$ is *given*, say $x_{1,0} = 0$. As a consequence we have with (18) $x_{4,0} = G_*$, and condition (38) is redundant. We also suppose that the control input $u(t)$ is *bounded*, i. e. :

$$0 \leq u(t) \leq U_{max} \tag{40}$$

where U_{max} is given.

Because the Hamiltonian H is *linear* in the control u, we know by Pontryagin's Minimum Principle[10] that our problem has become a *Bang–Singular–Bang* problem, i. e. :

$$u(t) = \begin{cases} U_{max} & \text{if } \psi < 0 \\ u_{sing} & \text{if } \psi = 0 \quad t_i \leq t \leq t_{i+1} \\ 0 & \text{if } \psi > 0 \end{cases} \tag{41}$$

On any *singular* interval $[t_i, t_{i+1}]$ the function ψ remains zero, so the Minimum Principle fails to provide the optimal solution. In that case, the *singular* control can be determined as follows. As $\psi = 0$ for all t in $[t_i, t_{i+1}]$, all of its derivatives with respect to t must vanish on the same interval, i. e. :

$$\frac{d^i \psi}{dt^i} = 0, \; i = 1, 2, \ldots, \text{ for all } t \text{ in } [t_i, t_{i+1}] \tag{42}$$

So we differentiate the function ψ repeatedly until u appears explicitly. We obtain successively :

$$\frac{d\psi}{dt} = \dot{\lambda}^{\mathrm{T}} \mathrm{b} = -\lambda^{\mathrm{T}} \frac{\partial \mathrm{f}}{\partial \mathrm{x}} \mathrm{b} \triangleq \lambda^{\mathrm{T}} \mathrm{d} = 0 \tag{43}$$

$$\frac{d^2\psi}{dt^2} = \dot{\lambda}^{\mathrm{T}} \mathrm{d} + \lambda^{\mathrm{T}} \frac{\partial \mathrm{d}}{\partial \mathrm{x}} \dot{\mathrm{x}} = -\lambda^{\mathrm{T}} \frac{\partial \mathrm{f}}{\partial \mathrm{x}} \mathrm{d} + \lambda^{\mathrm{T}} \frac{\partial \mathrm{d}}{\partial \mathrm{x}} (\mathrm{f} + \mathrm{b}u) = 0 \tag{44}$$

The last equation can be solved for u_{sing}:

$$u_{sing}(t) = \frac{\lambda^{\mathrm{T}}((\partial \mathrm{f}/\partial \mathrm{x})\mathrm{d} - (\partial \mathrm{d}/\partial \mathrm{x})\mathrm{f})}{\lambda^{\mathrm{T}}(\partial \mathrm{d}/\partial \mathrm{x})\mathrm{b}} \tag{45}$$

Note that in this case the denominator of the above expression is indeed different from zero. For obvious reasons, we call this problem a *singular problem of order 2.* We wish to emphasize that this quite compact expression represents a lot of analytic calculations on the right–hand side of equation (16), as the partial derivatives of first and second order with respect to all state variables are needed!

Note that both the numerator and the denominator are *linear* in the costate λ. We now show that on a singular interval, the optimal control is a *nonlinear feedback law of the state–variables only.* In order to do so, it is sufficient to find three linear homogeneous

equations in the *costate*–variables, so that any three of them could be solved in terms of the fourth one. These equations are :

$$\psi \equiv \lambda^T \mathbf{b} = 0 \tag{46}$$

$$\frac{d\psi}{dt} \equiv \lambda^T \mathbf{d} = 0 \tag{47}$$

as on the singular interval ψ and $d\psi/dt$ are zero by definition. The third equation follows then from the condition $H = 0$ for all t:

$$\phi \equiv \lambda^T \mathbf{f} = 0 \tag{48}$$

For this particular model, it can be seen that λ_4 has disappeared from u_{sing}, as $f_4 \equiv 0$. So the first equation can be omitted, and the last two could be solved as follows :

$$\begin{pmatrix} f_1 & f_2 \\ \beta_1 & \beta_2 \end{pmatrix} \begin{pmatrix} \lambda_1 \\ \lambda_2 \end{pmatrix} = - \begin{pmatrix} f_3 \\ \beta_3 \end{pmatrix} \lambda_3 \tag{49}$$

where

$$\beta_i \triangleq b_1 \frac{\partial f_i}{\partial x_1} + b_4 \frac{\partial f_i}{\partial x_4}, \; i = 1, \ldots, 3 \tag{50}$$

The conclusion is that the introduction of an upper limit on $u(t)$ and the specification of the complete initial state reduce the optimization problem to the determination of the *optimal sequence* and the corresponding *switching times*. Once this problem has been solved, we shall tackle the original problem by letting $U_{max} \rightarrow \infty$.

3.3 Computational algorithm

Our analysis is based on the work of Lim et al.[4], but we shall develop an algorithm without the need for any costate variable at all. The determination of the optimal sequence of *fed*– and *batch*–phases can be simplified a lot by thinking of the fermentation as a *biphasic* process, as many experiments have shown : the process starts with the *growth*–phase, to produce as much as possible biomass X, and continues with the *production*–phase, to produce product P as much as possible. The optimal switching time between these phases—given the total amount of input available for the fermentation— is obviously dictated by a *trade off* between the gain in product P by increasing the biomass X, and the gain in P by optimizing the specific production rate π. This can be seen readily from equation (12). In other words, during the first phase we shall pay attention to the specific growth rate μ, while during the production we shall focus on π. Observe that this reasoning is more or less independent of the specific expressions for μ and π.

We shall derive now the optimal control *sequence* in a more or less heuristic way, based on microbial insight. Some more mathematical evidence for the following line of reasoning shall be given later on. In the most general case of low initial values for S and X, it is clear that on $t = t_0$ the control must take on its maximum value $u = U_{max}$, as μ is monotonously

increasing with C_s. At some instant $t = t_1$, the control is set equal to its minimum value $u = 0$: this allows the substrate concentration C_s to reach its lower optimal value to start the production at $t = t_2$. The basic idea behind this is the following. During the production phase, we may expect π to be in the neighbourhood of its maximum value $Q_{p,max}$. As we focus on production and not on growth, it follows from equation (6)—or equivalently equation (29) with B near to 0—that μ shall have to decrease to the neighbourhood of $\mu = \mu_{crit}$. Obviously this can only be done by decreasing C_s. Whatever the optimal concentration C_s during production is—we shall see in Appendix 2 that in general it is time–varying—, we may expect that the quite specific $C_s(t)$–profile cannot be achieved by a simple *Bang–Bang* control. So at time $t = t_2$ the *singular* control u_{sing} must take over. As the final time t_f is free, we must look for another stopping condition. We remark that the total amount of input is fixed to α—equation (22), so the singular control is stopped when the terminal constraint $x_{4,f} = G_f$ (23) is met, say at time $t = t_3$. Remark that we have taken for granted that the upper bound U_{max} is never violated during singular control. As there may be still some substrate in the fermentor, the fermentation continues in batch–mode—$u = 0$—until dP/dt becomes 0, i. e. until the net penicillin formation rate becomes 0.

Let us first formulate some remarks. It should be noted that the time t_1 has a clear physical interpretation : $U_{max} \times t_1$ represents the amount of feed consumed in the growth–phase. Secondly, remember that the singular control is a nonlinear feedback law of the state variables only, so it is *not* necessary to guess any costate variable at $t = t_2$. The conclusion is that the introduction of mathematical and microbial insights into this particular problem has transformed the $TPBVP$ which is difficult to solve in general, into a simple two–dimensional optimization problem of switching times t_1 and t_2.

We now summarize the above developments in a straightforward computational algorithm :

- Make a guess of t_1, or equivalently, determine the amount of substrate reserved to the growth–phase.
- Make a guess of t_2. As we prove in Appendix 2, a good starting value is the time t for which $C_s(t)$ maximizes π/σ. Note that this value of C_s can be calculated *a priori*. When $B \approx 0$, this is equivalent to the time t for which $\mu = \mu_{crit}$ (see Appendix 2).
- Integrate the state equations using the above determined control sequence and store the value of the cost index $J(u)$ (21).
- For the same guess of t_1, refine the value of t_2 by considering $t_{2,new} = t_{2,old} \pm \delta t$, with δt as small as required. Save the time t_2 for which $J(u)$ reaches its minimum.
- Restart the procedure with a new guess of t_1 in order to minimize $J(u)$. For the problem at hand, a linear search method for t_1 has been chosen.

3.4 Optimal Control with unbounded input and some initial states free

Let us now return to the original problem, i. e. *no upper bound on the input $u(t)$, and $x_{1,0}$ and thus $x_{4,0}$ undetermined.* We show that in the above reasonings some minor modifications shall suffice. As a matter of fact, the upper limit U_{max} on the input—representing an upper bound on the feeding pumps—can be removed by installing more or larger pumps to deliver the requested influent flow rate.

Consider again the above control sequence. The only place where the upper limit U_{max} is active is in the time interval $[t_0, t_1]$. Suppose now that the value of U_{max} becomes larger. As a consequence, the value of t_1 shall decrease. In the limit, when $U_{max} \to \infty$, $t_1 \to 0$, and the control during growth becomes a *Dirac impulse on $t = 0^+$ with an intensity equal to the amount of substrate reserved to the growth.* This Dirac impulse in the origin can be replaced by an equivalent set of *initial conditions* with the same effects on future time histories of all states. In other words, omitting the upper bound on the input leads to the injection of all substrate reserved to growth at the beginning of the fermentation, the growth phase becoming a *batch*–phase. Of course this is the way to achieve the maximum amount of biomass X with a given amount of substrate, as C_s and thus μ take their highest possible values for all t during growth. The equivalent set of initial conditions for this case is :

$$\begin{cases} x_{1,0} \text{ which shall be optimized} \\ x_{4,0} = G_* + x_{1,0}/s_F \end{cases}$$

In the above computational algorithm, the only modification is to replace the time t_1 by the *equivalent* initial condition $x_{1,0}$. Note that these two variables have indeed the same physical interpretation mentioned earlier!

3.5 A related problem

We have now solved the given optimization problem as a limiting case of a *Bang–Singular–Bang* problem. Let us now look to a *third* related problem that can be solved with the same computational scheme. As we shall see in the simulations further on, the unconstrained optimization can give rise to a quite high initial value $x_{1,0}$ and thus $C_{s,0}$. In practice, this may lead to a lot of undesired effects, e. g. a *solubility* problem, an *inhibition* problem, unproductive *side–reactions*,...thus suggesting the need for an upper limit on C_s, say $C_{s,max}$. The best we can do in that case is to start the fermentation with $C_{s,0} = C_{s,max}$, or in other words :

$$x_{1,0} = \frac{s_F C_{s,max} G_*}{s_F - C_{s,max}} \tag{51}$$

$$x_{4,0} = \frac{x_{1,0}}{C_{s,max}} \tag{52}$$

During the growth–phase we then apply a control—a *Zulauff* [11] process—that keeps C_s on its maximum value $C_{s,max}$, thus assuring the highest possible value of μ. This control is

derived as follows. We must have :

$$\frac{dC_s}{dt} \equiv \frac{d(S/G)}{dt} = 0 \tag{53}$$

With equations (10) and (13) we obtain :

$$u_{growth} = \frac{s_F \sigma X}{s_F - C_{s,max}} \tag{54}$$

which is the desired control in closed–loop form. This control is terminated at time $t = t_1$, which has exactly the same meaning as mentioned above. We conclude that a state inequality constraint of the form

$$C_s(t) \equiv \frac{S(t)}{G(t)} \leq C_{s,max} \tag{55}$$

introduces no additional complication in the developed numerical scheme.

3.6 Mathematical justification of the proposed algorithm

Before giving some simulation results, let us pay some more attention to the mathematical justification of the derived control schemes. As an example, we shall treat the original problem—no constraints on u or C_s.

We know that along an extremal trajectory the Hamiltonian $H = 0$ for all t. Since—as indicated by the developed control scheme—the product $\psi(t)u(t) = 0$ for all t, we also have $\phi(t) = 0$ for all t. At the terminal time t_f, we obtain with (33) and (37):

$$f_3(t_f) = 0 \tag{56}$$

or in other words:

$$\frac{dP}{dt} = 0 \tag{57}$$

a result we have already derived from physical arguments.

An extremal trajectory is completely defined by the couple $(\hat{S}_0, \hat{t}_2)$—the superscript "$\hat{}$" denotes values obtained with our algorithm. The unknown times $\hat{t}_3$ and $\hat{t}_f$ result then from a simulation. In fact we must verify, for such a trajectory to be an extremal one, that *all* necessary conditions are fulfilled. As we already mentioned, we did not make any use of the costate vector $\lambda(t)$ in the computational algorithm.

Therefore, the following conditions must be satisfied by the trajectory generated by $(\hat{S}_0, \hat{t}_2)$:

- at $t = t_f$, the costate $\lambda(t_f)$ must satisfy the boundary conditions (37).
- the Hamiltonian H must be equal to zero along the whole trajectory, or in other words:

$$\begin{array}{rcll} \phi & = & 0 & \text{for all } t \\ \psi & = & 0 & \text{on the singular interval} \\ \psi & > & 0 & \text{for all } t \text{ where } u(t) = 0 \end{array}$$

Let us describe now how to verify these conditions efficiently. Suppose for some $\hat{S}_0$ we have found the corresponding $\hat{t}_2$ with the above algorithm.

- As a simulation result we obtain $\hat{t}_3$ and $\hat{t}_f$ together with $\mathrm{x}(\hat{t}_2)$, $\mathrm{x}(\hat{t}_3)$ and $\mathrm{x}(\hat{t}_f)$.
- At $t = \hat{t}_3$, the control switches from $u(\hat{t}_3^-) = u_{sing}$ to $u(\hat{t}_3^+) = 0$. This causes a jump in $\dot{\mathrm{x}}(t_3)$, but all states and costates remain continuous. Therefore, we can approach $\hat{t}_3$ from the left and calculate all costates from the singular conditions.
  - the third equation of the costate–system (35) together with the third terminal condition (37) delivers:
    $$\lambda_3(t) = -e^{k_h(t-\hat{t}_f)} \tag{58}$$
    so $\lambda_3(\hat{t}_3)$ is known.
  - $\lambda_1(\hat{t}_3)$ and $\lambda_2(\hat{t}_3)$ follow then from (49), $\lambda_4(\hat{t}_3)$ follows from (46).
- Integrate the state–equations (16) together with the costate–equations (35) using (58) from $\hat{t}_3$ to $\hat{t}_f$ with $u(t) = 0$. Verify if $\phi(t) = 0$ and $\psi(t) > 0$. Verify also the terminal conditions (37) on the costate.
- Along the singular interval $[\hat{t}_2, \hat{t}_3]$ we calculated the complete costate out of $\phi = 0$ and $\psi = 0$, so $H = 0$ by definition. We obtain the costate on $t = \hat{t}_2$ in the same way as on $t = \hat{t}_3$.
- Integrate the state–equations (16) together with the costate–equations (35) using (58) backwards in time from $\hat{t}_2$ to $t_0 = 0$ with $u(t) = 0$. Verify if $\phi(t) = 0$ and $\psi(t) > 0$. Verify also all conditions on $t = t_0$.

Note that the above conditions could be seen as a test on the accuracy of $\hat{t}_2$ for a given $\hat{S}_0$. It should be clear that the number of extremal solutions is in fact infinite : one for every $\hat{S}_0$ considered fixed.

We shall now consider the question whether an *extremal* trajectory is *optimal*. Suppose—as we shall demonstrate further on—there exists a *unique, optimal* couple (S_0^*, t_2^*). Consider then $\hat{S}_0$ in the neighbourhood of S_0^* as a *fixed* initial state. Then we know that condition (38) is redundant as the complete initial state $\mathrm{x}(t_0)$ is known. If we determine the corresponding $\hat{t}_2$ with the above algorithm, then the resulting trajectories $(\hat{\mathrm{x}}, \hat{\lambda}, \hat{u})$ shall satisfy all necessary conditions, in particular—as a test on the accuracy of $\hat{t}_2$—the Hamiltonian H must vanish along the solution. The conclusion is that for $\hat{S}_0$ *fixed* in the neighbourhood of S_0^*, the extremal control $\hat{u}(t)$ obviously is the *unique, optimal* control, as there are no degrees of freedom except t_2!

Of course, we have tacitly assumed that the previously determined *control sequence Batch–Singular–Batch* is the optimal one. This is correct, because :

- the last phase must be a batch–phase, as we have shown above.

- there is only one singular interval $[t_2, t_3]$, which cannot be left unless the isoperimetric constraint (22) on u is met. In other words, the singular control is *not* interrupted by e. g. a batch–phase. This can be explained as follows. Suppose the hydrolysis $k_h = 0$. Then it is not difficult to prove that the singular control keeps C_s on a constant value, e. g. for $B = 0$ $C_s = C_{s,crit}$ corresponding to μ_{crit}—see Appendix 2. Any batch–phase shall move the state away from the *singular hyperplane*, and it may even cause dP/dt to become negative. To bring the state back to the optimal production conditions $C_s = C_{s,crit}$, i. e. to the singular hyperplane, it shall take a certain amount of control energy which is then lost for the production itself, thus resulting in a higher value of the cost $J(u)$. For hydrolysis k_h positive, Appendix 2 tells us that C_s is not constant during singular control. However, it is clear that the above line of reasoning shall still hold, noting that a batch–phase always generates a decrease in C_s.

- it is in fact possible that for some $\hat{S}_0$, the switching time $\hat{t}_2$ is equal to 0. In other words the initial state lies on the singular surface, and the production may start immediately. Obviously, this shall be detected correctly by the proposed algorithm, as it is only a special case of the derived control sequence.

Keeping in mind that the number of extremal solutions is infinite, how can we detect the *optimal* solution for the problem with a *free* S_0 ? We propose two methods to determine the *optimal* S_0^* and then the optimal control. As a first method, one could make use of the necessary condition (38). The optimal S_0^* obviously is the one for which this condition is satisfied. However this approach has some drawbacks :

- the costate $\lambda(t)$ must be calculated for *every* guess of S_0 and t_2. This can be done with the method we described above, but it implies a lot of additional computational work.

- extensive simulations have shown that the calculation of the costate on $t = t_0$ poses some numerical difficulties. As a matter of fact, the proposed condition seems to be a bad criterion to detect the optimal solution.

Therefore, in the last step of our algorithm, we simply look at the *cost index* $J(u)$ itself. Simulation has shown (see Section 3.4) that the relation $J(u)$ versus S_0 looks like a quadratic function, so that its optimum could be detected by e. g. a simple *linear search method* for S_0. Another consequence of this quadratic behaviour is that we are able to find a *global optimum* for this problem!

3.7 Simulation results

Remember that the aim of this paper is to verify the statement of Heijnen et al. that *the glucose feed strategy is of crucial importance in obtaining high penicillin yields.* This statement was based on the following set of controls : a constant input, a linearly increasing input and a linearly decreasing input. The initial state was fixed, the final time and the

total amount of substrate were fixed too. The next table summarizes the results we have obtained using the *NAG*–routine *D02EHF*.

Operational conditions			
S_0	5500	P_0	0
X_0	4000	G_0	100000
t_f	200	α	205500
Control $u(t)$			P_f
$u(t) = 1000$			3001.
$u(t) = 500 + 5t$			5883.
$u(t) = 1500 - 5t$			89.

Table 2 *Simulation results with the controls of Heijnen et al.*

Although Heijnen et al. did not consider other feeding strategies, the above results indicate that the present model allows for the optimization of the glucose feed rate scheme with respect to the final amount of product P_f.

Let us present now some results obtained with our algorithm. We shall focus on $B = 10^{-11}$ as an approximation of the original *Blackman* model, and on the other extreme $B = 10^{-2}$ where $\pi(\mu)$ becomes a *Monod*–law.

In Figure 4, we have visualized the actions taken by the described optimization algorithm for $B = 10^{-11}$. For every S_0, we determine the optimal t_2. As a consequence, we obtain the corresponding values for $P(t_f)$ and t_f. Clearly, the optimal couple (S_0^*, t_2^*) is the one which maximizes $P(t_f)$. Observe the quadratic behaviour of $P(t_f)$ as a function of S_0, so we have indeed a *unique optimal* solution for this problem.

Figure 4 *Extremal values for* $P(t_f)$, t_2 *and* t_f *as functions of* S_0 *for* $B = 10^{-11}$

Note that there exists a lower limit S_{min} on the possible values for S_0, corresponding to $t_2 = 0$. In that case, the complete state lies on the singular hyperplane, so singular control starts immediately.

The results for S_0 near to its maximum value α are presented in the following table:

S_0	t_2	t_3	t_f	P_f
200000	68.064	69.373	69.440	2962.88
205000	68.384	68.501	68.568	2795.38
205500	68.482	68.482	68.482	2778.63

Table 3 *Extremal values for* S_0 *near* α *for* $B = 10^{-11}$

We note that the last row corresponds to a complete *batch*–fermentation : $t_f \equiv t_3 \equiv t_2$. For every t, $u(t) = 0$. Remark also that even for these large values of S_0, the condition $dP/dt = 0$ is never met *before* $t = t_2$, so we can indeed apply our algorithm to the whole possible range $[S_{min}, \alpha]$ for S_0. As a consequence, the initial guess for S_0 may be far from the optimal one. Some numerical values for the optimal control are:

G_0	99100	t_2	22.321
S_0	3000	t_3	349.987
X_0	4000	t_f	350.101
P_0	0	P_f	8319.461

Table 4 *Optimal Control results for* $B = 10^{-11}$

Figure 5 *Optimal glucose feed rate and corresponding cell, glucose, product,* π *and* μ *profiles for* $B = 10^{-11}$

Figure 5 shows the corresponding time profiles. Let us draw the following remarks. First of all, we note that the initial amount S_0 is rather low, resulting in a small batch–phase of 22.32 hrs. In fact the singular interval takes most of total fermentation time. The terminating batch–phase is negligible small. From the profiles for $X(t)$ and $P(t)$ we conclude that, although the optimal control algorithm is based on the conjecture of a *biphasic* process, this biphasic behaviour has disappeared almost completely, compared with e. g. the results for the *constant* strategy of Figure 3. Principally this is due to the structure of the specific production rate π, which makes it possible to produce at the highest specific production rate for $\mu \geq \mu_{crit}$, in other words the production is assumed to be *growth–associated.*

Remark that on the singular arc, the control seems to maintain μ at the lowest possible value—i. e. μ_{crit}—which still guarantees the maximum value for π. In fact we know that during singular control $C_s(t)$—and thus $\mu(t)$ and $\pi(t)$—are time–varying as $k_h \neq 0$—see Appendix 2. However, k_h is so small that the resulting variations in C_s—and thus in μ and π—are in fact negligible so that they cannot be detected on this plot. The preceding batch–phase is used to bring μ to its optimal value for production. It is important to see that the optimal control keeps π on its highest value for all $t < t_3$. This shall be the basis for the construction of *suboptimal* profiles in the next section.

In order to evaluate the performance of the Optimal Control $u^*(t)$, we need some *reference.* As we do not penalize the total fermentation time t_f in the cost $J(u)$, a good choice might be a *constant* control with $t_f = t_f^*$, t_f^* denoting the optimal fermentation time. As for convenience, we take $S_0 = 0$ mol. Then we define a *gain* γ as follows :

$$\gamma(u^*) \triangleq 100 \times \frac{J(u^*) - J(u_{ref})_{t_f = t_f^*}}{J(u_{ref})_{t_f = t_f^*}} \ \% \tag{59}$$

For $B = 10^{-11}$, a constant control during 350.101 hrs with $S_0 = 0$ produces 1981.283 mol penicillin. So for the Optimal Control $u^*(t)$ we obtain a *gain* of 319.9 %! Remark the enormous increase in the final amount P_f, which may suggest some questions concerning the validity of the model of Heijnen et al. As up to now the penicillin–fermentation has been recognized through all experiments as an intrinsically *biphasic* process, it seems somewhat unlikely that the obtained control put into practice would result in a quasi *monophasic* fermentation, producing such a high gain. We conclude that the obtained results suggest some possible shortcomings in the model we have used in this work. A deeper study of this model in comparison with the model of Bajpai and Reuß[2] is the subject of another paper[7].

We now give the analogous results for the other extreme $B = 10^{-2}$, in order to demonstrate that the developed algorithm can be applied to *every* model with B between $0 < B \leq \mu_{crit}$. Figure 6 shows the evolution of t_2, and thus $P(t_f)$ and t_f, as functions of S_0. Remark that the optimal couple (S_0^*, t_2^*) corresponds to $t_2 = 0$, in other words the optimal initial state lies on the singular hyperplane itself. As a consequence, the separation between *growth*- and *production*-phase has disappeared completely. This is also illustrated by the time profiles of Figure 7.

Figure 6 *Extremal values for $P(t_f)$, t_2 and t_f as functions of S_0 for $B = 10^{-2}$*

Note that in this case the lower limit S_{min} is equal to the optimal value S_0^*. The following table shows the results for S_0 near to its maximum value α :

S_0	t_2	t_3	t_f	P_f
200000	67.833	69.114	69.184	2505.80
205000	68.152	68.267	68.335	2442.59
205500	68.252	68.252	68.252	2436.26

Table 5 *Extremal values for S_0 near α for $B = 10^{-2}$*

Note again that the condition $dP/dt = 0$ is never met *before* $t = t_2$, so we can indeed apply our algorithm to the whole possible range $[S_{min}, \alpha]$ for S_0.

Some numerical values for the optimal control are:

G_0	98137.36	t_2	0
S_0	326	t_3	277.205
X_0	4000	t_f	277.320
P_0	0	P_f	4564.455

Table 6 *Optimal Control results for $B = 10^{-2}$*

Figure 7 *Optimal glucose feed rate and corresponding cell, glucose, product, π and μ profiles for $B = 10^{-2}$*

Remark that on the singular arc, the variations of π and μ and thus of C_s with respect to time are more pronounced, although k_h has not been changed. We conclude that the *model structure* itself plays also an important role in the amplitude of these variations.

A *constant* strategy during 277.320 hrs with $S_0 = 0$ mol produces 1978.425 mol penicillin, so the gain for this case is $\gamma = 130.7$ %.

As mentioned above, we could repeat these calculations for every B within the given boundaries. The result for the optimal production P_f is shown in Figure 8, as an illustration of the basic conjecture of Section 2. From this plot we conclude that the sequence of optimal controls $u(B,t)$ is indeed convergent. Note also that for $B < 10^{-9}$ the cost has almost reached its limit value.

Figure 8 *Optimal production P_f as a function of B*

4 A heuristic control strategy

4.1 Derivation of suboptimal profiles

In this section, we propose a *heuristic* control based on mathematical and microbial knowledges. Some of the ideas are reported elsewhere[5,12]. We shall show that under certain conditions this control coincides with the *optimal* one.

As there is no need for partial derivatives, the original model can be handled directly without any difficulties. So let us begin with $B = 0$. Later on, we shall evaluate the results for B in $0 < B \leq \mu_{crit}$.

The construction of a suboptimal profile is based principally on the concept of a *biphasic* fermentation. For the control during *growth*, we refer to the previous section : all substrate consumed for growth is added all at once at $t = 0$ in order to obtain the highest possible value of μ. Remark that for the given specific production rate (6) this results in maximizing π also. During *production*, we focus on the specific rate π. Equation (6) indicates that the lowest value of μ which still guarantees the maximum value of π is $\mu = \mu_{crit}$. Note that this is equivalent to $C_s = C_{s,crit}$, so the control during production is of the form:

$$u_{production} = \frac{s_F \sigma X}{s_F - C_s} \tag{60}$$

maintaining C_s and thus μ on their critical values. As a consequence, the conjunction point t_2 of growth and production is simply dictated by the condition:

$$C_s = C_{s,crit} \qquad \text{or} \qquad \mu = \mu_{crit} \tag{61}$$

The control is stopped at $t = t_3$ when all substrate is used. As in the optimal case, the concluding batch-phase is stopped whenever $dP/dt = 0$.

Observe that this suboptimal control sequence agrees very well with the optimal one : the only change is the substitution of the *singular control* by the above control that keeps C_s and thus μ constant. Note also that the complete suboptimal control is obtained in *closed-loop* for a given S_0. As a result, the optimization problem is reduced to the *one-dimensional optimization of* S_0.

It should be clear from the previous section and Appendix 2 that for $B = 0$ and $k_h = 0$ this *heuristic control coincides with the optimal one.*

For values of B in the interval $0 < B \leq \mu_{crit}$ it is less clear how to determine a heuristic control during production as the specific production rate π (29) has no *corner point* anymore. However, we shall still keep C_s and thus μ *constant* using a control of the form (60).

The switching from growth to production could be determined as follows. As a first guess, we can still switch on $C_s = C_{s,crit}$ and thus $\mu = \mu_{crit}$. However, we know from Appendix 2 and Figure 15 that this guess is only appropriate for B near 0. For B near μ_{crit}, we shall simply optimize the switching time t_2, so we obtain again a *two-dimensional optimization of* S_0 *and* t_2.

Before giving some simulation results, let us first mention some advantages of these suboptimal profiles. It is well–known that putting an *optimal control* into practice may be hampered by a lot of problems. If the control law is not obtained in complete closed–loop form—as is the case here—, it cannot compensate for unmodeled disturbances, parameter variations, ... Further on, as Optimal Control is a very model–sensitive technique, a *feed-forward* shall not generate the predicted results. As long as a sufficiently accurate model for the penicillin fermentation is not available, the determined profiles can be used only to obtain a greater qualitative insight in the process.

On the other hand, the *suboptimal* profiles we present here are the translation of a more realistic control objective, namely *setpoint* control, for which even adaptive control algorithms can be developed. As suggested by e.g. Dochain et al.[13], one could keep μ constant *without* the knowledge of an exact analytic expression for it, so the algorithm becomes model–independent. Further on, there would be no need for a complete measurement of the state, a problem which has not been solved completely up to now.

4.2 Simulation results

First we present some results for $B = 10^{-11}$, in other words for the original model. Figure 9 presents the time profiles for the different variables. Some numerical values are indicated in the following table:

G_0	99100	t_2	22.337
S_0	3000	t_3	350.037
X_0	4000	t_f	350.151
P_0	0	P_f	8319.239

Table 7 *Suboptimal Control results for* $B = 10^{-11}$

Figure 9 *Suboptimal glucose feed rate and corresponding cell, glucose, product,* π *and* μ *profiles for* $B = 10^{-11}$

Figure 10 *Suboptimal and Optimal glucose feed rate for* $B = 10^{-11}$

Figure 10 compares the suboptimal and optimal control profiles. We conclude that for the original model, the suboptimal control results almost coincide with the optimal values, thanks to the low value of k_h.

For $B = 10^{-2}$, i. e. $\pi(\mu)$ *Monod*, the results are summarized in Table 8 and Figures 11 to 13. We have done the optimization with both $\mu_{switch} = \mu_{crit}$ and μ_{switch} considered *free*.

$\mu_{switch} = \mu_{crit}$			
G_0	100540	t_2	29.573
S_0	7000	t_3	292.890
X_0	4000	t_f	292.995
P_0	0	P_f	4399.589
μ_{switch} *free*			
G_0	98380	t_2	12.225
S_0	1000	t_3	304.665
X_0	4000	t_f	304.792
P_0	0	P_f	4553.437

Table 8 *Suboptimal Control results for* $B = 10^{-2}$

Figure 11 *Suboptimal glucose feed rate and corresponding cell, glucose, product,* π *and* μ *profiles for* $B = 10^{-2}$ *and* $\mu_{switch} = \mu_{crit}$

Figure 12 *Suboptimal glucose feed rate and corresponding cell, glucose, product,* π *and* μ *profiles for* $B = 10^{-2}$ *and* μ_{switch} *free*

Figure 13 *Suboptimal and Optimal glucose feed rate for* $B = 10^{-2}$

Note that—in contrast with the *optimal* profile—for both suboptimal profiles there is still an initial batch–phase. For $\mu_{switch} = \mu_{crit}$ the final amount P_f reaches 96.39 % of the optimal value. For μ_{switch} considered *free* we obtain even 99.77 %! These results sufficiently illustrate the value of the developed suboptimal profiles for the whole range of B.

Before formulating some conclusions we first give a final remark. Although the only model reported in the literature is the one with $B = 0$, we still mentioned some simulation results for other values of B. First of all, from the biochemical point of view a sharp corner in π at $\mu = \mu_{crit}$ is of course only a first approximation of real life fermentation conditions. So a value for B different from zero seems more realistic. Secondly, these results make it possible to illustrate the convergence of the controls to the desired one following the basic conjecture of Section 2, see e.g. Figure 8. Finally, they confirm the use of the developed algorithms for optimal and suboptimal control not only for the original model, but for a whole class of fermentation processes.

5 Conclusions

As mentioned in the introduction, the principal purpose of this paper was to present a methodology in order to determine Optimal Control profiles for a certain class of piecewise smooth models that cannot be handled in a direct way. As an example, the mathematical model for the penicillin G fermentation of Heijnen et al. has been studied. As this kind of models is not limited to the biotechnological field itself, it is clear that this procedure can be of great use in a lot of other scientific domains. Further, we were able to include the optimization of some initial states by considering the given optimization problem as a limiting case of a problem with bounded input and fixed initial state. We believe that this work has given also a contribution to three other fields.

First of all, we verified the statement by Heijnen et al. that the *glucose feed scheme is of crucial importance in obtaining high penicillin yields.* In order to do so, we determined for the first time the Optimal Control profile for a well–defined optimization problem using their model. We have shown that the obtained control generated the global optimum of the performance measure we have considered. Simulation results indicate a possible gain of several hundreds percents compared with a constant control input with zero initial substrate amount !

Secondly, on the field of *model building*, the obtained results indicated some possible shortcomings in the model used, without carrying out any costly and time–consuming experiments. The combination of the enormous gains in production and the vanishing of the characteristic biphasic behaviour through optimization, made us conclude that the present model might be less useful for advanced control purposes than suggested by Heijnen et al. However, we were able to prove some theorems for a quite large class of kinetics, characterizing the singular control.

Finally, we presented a *heuristic control* strategy based on mathematical and microbial knowledge that proved to be a successful alternative for the optimal control, for the whole family of models we considered in this paper. We derived the conditions for which this heuristic strategy coincides with the optimal control. It was pointed out that the suboptimal controls can be calculated using essentially the same algorithm as for the optimal profiles. This heuristic methodology is in fact the translation of a more realistic control objective, namely setpoint control. It opens perspectives for the development of more reliable and even model–independent control schemes.

A Appendix 1

In this appendix we derive some boundary conditions if the initial state is not given in an explicit way.

Consider a continuous dynamic system described by:

$$\dot{\mathrm{x}} = \mathrm{f}(\mathrm{x}, \mathrm{u}, t) \tag{62}$$

Let $J(u)$ be the cost index to be minimized:

$$J(u) = g(\mathrm{x}(t_f), t_f) + \int_{t_0}^{t_f} L(\mathrm{x}, \mathrm{u}, t)dt \tag{63}$$

Then $\overline{J}(u)$ denotes the *augmented* cost, i. e. the cost to which the system differential equations have been adjoined using multiplier functions $\lambda(t)$:

$$\overline{J}(u) \triangleq J(u) + \int_{t_0}^{t_f} \lambda^{\mathrm{T}}(t)(\mathrm{f}(\mathrm{x}, \mathrm{u}, t) - \dot{\mathrm{x}})dt \tag{64}$$

Now consider the *variation* in $\overline{J}(u)$ due to *admissible* variations in the control vector $u(t)$ for fixed time t_0—see Reference 14 :

$$\delta\overline{J}(u) = \lambda^{\mathrm{T}}(t_0)\delta\mathrm{x}(t_0) + \ldots \tag{65}$$

where only terms on $t = t_0$ are mentioned. For an extremum, $\delta\overline{J}$ must be zero for any admissible $\delta u(t)$. Remark that the range of admissible control variations $\delta u(t)$ is *not* influenced by any constraint on the initial state $\mathrm{x}(t_0)$. As a consequence, all necessary conditions on times $t > t_0$ to make $\delta\overline{J}(u)$ vanish, shall still hold independently of the constraints on $\mathrm{x}(t_0)$.

For a *fixed* initial state $\mathrm{x}(t_0)$, we have $\delta\mathrm{x}(t_0) = 0$ and the term disappears from $\delta\overline{J}$. For a *free* initial state, there shall be an optimal value for $\mathrm{x}(t_0)$ such that $\delta\overline{J} = 0$ for arbitrarily small variations of $\mathrm{x}(t_0)$ around this value. As a consequence, we must choose:

$$\lambda(t_0) = 0 \tag{66}$$

Of course, for some initial state $x_i(t_0)$ unspecified, the others given, we must have the corresponding $\lambda_i(t_0) = 0$.

Suppose that on $t = t_0$ the initial states are only determined by a set of constraints of the form:

$$\mathrm{h}(\mathrm{x}(t_0)) \triangleq \begin{pmatrix} h_1(\mathrm{x}(t_0)) \\ \vdots \\ h_k(\mathrm{x}(t_0)) \end{pmatrix} = 0 \tag{67}$$

Clearly, $k \leq n$ where n denotes the dimension of the state x. We suppose n to be greater than 1, as for $n = 1$ the initial state is completely defined by the scalar equation $h(x(t_0)) = 0$. Remark that for $k = n$ the initial state is also completely determined by

the given constraints. For $k > n$ there are $(k-n)$ redundant conditions. So we focus on the case $k < n$, where we have to find $(n-k)$ additional conditions on $t = t_0$. These are derived as follows.

Introducing a $k \times 1$ vector ν of constant Lagrange–multipliers, we adjoin the constraints to the augmented cost function—for simplicity we shall use the same notation $\overline{J}(u)$—to obtain:

$$\overline{J}(u) = \lambda^{\mathrm{T}}(t_0)\mathrm{x}(t_0) + \nu^{\mathrm{T}}\mathrm{h}(\mathrm{x}(t_0)) + \dots \tag{68}$$

As before, we only concentrate on terms at $t = t_0$. Then the first variation of the cost becomes:

$$\delta\overline{J}(u) = (\lambda^{\mathrm{T}}(t_0) + \nu^{\mathrm{T}}\frac{\partial \mathrm{h}}{\partial \mathrm{x}}(t_0))\delta\mathrm{x}(t_0) + \dots \tag{69}$$

where $\partial\mathrm{h}/\partial\mathrm{x}$ denotes the $k \times n$ Jacobian matrix. Obviously, to make the term in $\delta\mathrm{x}(t_0)$ disappear, we must choose:

$$\lambda(t_0) + \frac{\partial \mathrm{h}}{\partial \mathrm{x}}^{\mathrm{T}}(t_0)\nu = 0 \tag{70}$$

These are n equations to determine the k Lagrange–multipliers ν_i and the $(n-k)$ additional boundary conditions.

As an example, consider the optimization problem given in the text. We have:

$$\begin{aligned} x_2(t_0) &= x_{2,0} \\ x_3(t_0) &= x_{3,0} \\ x_4(t_0) &= G_* + x_1(t_0)/s_F \end{aligned}$$

So the vector h for this case is—$n = 4$ and $k = 3$:

$$\mathrm{h}(\mathrm{x}(t_0)) \triangleq \begin{pmatrix} x_2(t_0) - x_{2,0} \\ x_3(t_0) - x_{3,0} \\ x_4(t_0) - x_1(t_0)/s_F - G_* \end{pmatrix} = 0 \tag{71}$$

and we obtain:

$$\begin{pmatrix} \lambda_1(t_0) \\ \lambda_2(t_0) \\ \lambda_3(t_0) \\ \lambda_4(t_0) \end{pmatrix} = - \begin{pmatrix} 0 & 0 & -1/s_F \\ 1 & 0 & 0 \\ 0 & 1 & 0 \\ 0 & 0 & 1 \end{pmatrix} \begin{pmatrix} \nu_1 \\ \nu_2 \\ \nu_3 \end{pmatrix} \tag{72}$$

Or, in other words:

$$\lambda_1(t_0) + \lambda_4(t_0)/s_F = 0 \tag{73}$$

which is the additional equation we are looking for. Remark that ν_1 and ν_2, and thus $\lambda_2(t_0)$ and $\lambda_3(t_0)$ remain undetermined, as $x_2(t_0)$ and $x_3(t_0)$ are given explicitly! ν_3 is only implicitly needed.

B Appendix 2

This appendix summarizes some properties of the singular control of the problem handled in the text.

We consider a fermentation process described by the following equations :

$$\frac{d\mathrm{x}}{dt} = \mathrm{f}(\mathrm{x}) + \mathrm{b}u \tag{74}$$

where

$$\mathrm{x} = \begin{pmatrix} x_1 \\ x_2 \\ x_3 \\ x_4 \end{pmatrix} \triangleq \begin{pmatrix} S \\ X \\ P \\ G \end{pmatrix} \tag{75}$$

and

$$\mathrm{f} = \begin{pmatrix} f_1 \\ f_2 \\ f_3 \\ f_4 \end{pmatrix} \triangleq \begin{pmatrix} -\sigma X \\ \mu X \\ \pi X - k_h P \\ 0 \end{pmatrix} \qquad \mathrm{b} = \begin{pmatrix} b_1 \\ b_2 \\ b_3 \\ b_4 \end{pmatrix} \triangleq \begin{pmatrix} 1 \\ 0 \\ 0 \\ 1/s_F \end{pmatrix} \tag{76}$$

The cost index is given by :

$$J(u) = g(\mathrm{x}(t_f)) \triangleq -P(t_f) \tag{77}$$

where the final time t_f is free. For the complete set of constraints and an explanation of all symbols used, we refer to the text.

The specific rates are specified as follows :

$$\sigma = Q_{s,max}\frac{C_s}{K_s + C_s} \tag{78}$$

For $0 < B < \mu_{crit}$ we have :

$$\pi(\mu) = Q_{p,max}\frac{(\mu + \mu_{crit}) - \sqrt{(\mu + \mu_{crit})^2 - 4(\mu_{crit} - B)\mu}}{2(\mu_{crit} - B)} \tag{79}$$

which reduces for $B = \mu_{crit}$ to :

$$\pi(\mu) = Q_{p,max}\frac{\mu}{\mu_{crit} + \mu} \tag{80}$$

$$\mu = Y_{x/s}(\sigma - m_s - \pi/Y_{p/s}) \tag{81}$$

It was shown in the text that within the given boundaries of parameter B, σ, μ and π are continuous, smooth functions of $C_s \equiv S/G$. For $B = 0$ we obtain the model of Heijnen et al.—with the simplified G–equation. We now prove the following theorem, which is a generalization of a result obtained by Modak et al.[15].

Theorem 1 *Consider the given system* (74) *with performance index* (77). *Suppose that* σ, μ *and* π *are functions of the substrate concentration* C_s *only, with continuous derivatives up to second order. Suppose also that the maintenance coefficient* m_s *is strictly positive. Then during singular control, the substrate concentration remains constant if and only if the hydrolysis* $k_h = 0$. *This constant value maximizes the yield* π/σ.

PROOF
In the following, a prime denotes derivation with respect to substrate concentration. The Hamiltonian H is given by :

$$H = \phi + \psi u \equiv 0 \tag{82}$$

where

$$\phi = (-\lambda_1\sigma + \lambda_2\mu + \lambda_3\pi)x_2 - \lambda_3 k_h x_3 \tag{83}$$

and

$$\psi = \lambda_1 + \lambda_4/s_F \tag{84}$$

The adjoint equations can be written as follows :

$$\dot{\lambda}_1 = (\lambda_1\sigma' - \lambda_2\mu' - \lambda_3\pi')x_2/x_4 \tag{85}$$

$$\dot{\lambda}_2 = \lambda_1\sigma - \lambda_2\mu - \lambda_3\pi = -(\phi + \lambda_3 k_h x_3)/x_2 \tag{86}$$

$$\dot{\lambda}_3 = \lambda_3 k_h \tag{87}$$

$$\dot{\lambda}_4 = -(\lambda_1\sigma' - \lambda_2\mu' - \lambda_3\pi')x_1x_2/x_4^2 \tag{88}$$

On the singular interval, we know that $\phi = 0$, $\psi = 0$ and $\dot{\psi} = 0$, or :

$$-\lambda_1\sigma + \lambda_2\mu + \lambda_3\pi = \lambda_3 k_h x_3/x_2 \tag{89}$$

$$\lambda_1 + \lambda_4/s_F = 0 \tag{90}$$

$$(\lambda_1\sigma' - \lambda_2\mu' - \lambda_3\pi')(1 - \frac{1}{s_F}\frac{x_1}{x_4}) = 0 \tag{91}$$

The case $x_1/x_4 \equiv C_s = s_F$ can be excluded as C_s is then unrealistic high during production. So the last equation is equivalent to :

$$\lambda_1\sigma' - \lambda_2\mu' - \lambda_3\pi' = 0 \tag{92}$$

Substituting these relations in the adjoint equations, one finds—with C_i a *constant* number:

$$\lambda_1 = C_1 \tag{93}$$

$$\dot{\lambda}_2 = -k_h\lambda_3 x_3/x_2 = -\dot{\lambda}_3 x_3/x_2 \tag{94}$$

$$\lambda_3 = -e^{k_h(t-t_f)} \tag{95}$$

$$\lambda_4 = C_4 \tag{96}$$

Remark that the differential equation for λ_3 has been solved with the boundary condition $\lambda_3(t_f) = -1$ due to the given performance index. As we know from the optimal control sequence that the product $\psi(t)u(t) = 0$ for all t, it follows from (82) that $\phi = 0$ for all t, so equation (94) holds for all t, with boundary condition $\lambda_2(t_f) = 0$ due to (37).

For the complete costate to be constant on the singular interval, obviously it is *necessary and sufficient* that the hydrolysis $k_h = 0$.

We now evaluate $d^2\psi/dt^2 = 0$ on the singular interval. We obtain after some calculations :

$$\dot{C}_s = k_h \frac{\lambda_3(\pi' x_2 - \mu' x_3)}{x_2(\lambda_1\sigma'' - \lambda_2\mu'' - \lambda_3\pi'')} \tag{97}$$

$$= -\sigma\frac{X}{G} + \frac{u_{sing}}{s_F G}(s_F - C_s) \tag{98}$$

the second equality due to the system–equations (74). Let us first verify that the denominator in equation (97) is different from zero. We shall give a demonstration by contradiction. So suppose that:

$$\lambda_1\sigma'' - \lambda_2\mu'' - \lambda_3\pi'' = 0 \tag{99}$$

Then together with equations (89) and (92) we obtain the homogeneous system :

$$\begin{pmatrix} -\sigma & \mu & \pi - k_h x_3/x_2 \\ -\sigma' & \mu' & \pi' \\ -\sigma'' & \mu'' & \pi'' \end{pmatrix} \begin{pmatrix} \lambda_1 \\ \lambda_2 \\ \lambda_3 \end{pmatrix} = \begin{pmatrix} 0 \\ 0 \\ 0 \end{pmatrix} \tag{100}$$

We know there exists a nontrivial solution $\lambda(t)$ since at least $\lambda_3(t) \neq 0$. So for assumption (99) to be true, a necessary and sufficient condition is that the above system–matrix has its determinant equal to zero. We have with (81) :

$$A \triangleq \begin{pmatrix} -\sigma & \mu & \pi - k_h x_3/x_2 \\ -\sigma' & \mu' & \pi' \\ -\sigma'' & \mu'' & \pi'' \end{pmatrix} = \begin{pmatrix} -\mu/Y_{x/s} - m_s - \pi/Y_{p/s} & \mu & \pi - k_h x_3/x_2 \\ -\mu'/Y_{x/s} - \pi'/Y_{p/s} & \mu' & \pi' \\ -\mu''/Y_{x/s} - \pi''/Y_{p/s} & \mu'' & \pi'' \end{pmatrix} \tag{101}$$

Obviously, A has no zero rows or columns, nor any identical rows or columns. The only possibility for $det(A)$ to be zero is that *both* k_h and m_s are zero, which is in contradiction with $m_s > 0$.

From equation (97) we conclude immediately that a necessary and sufficient condition for C_s to be constant on the singular interval is $k_h = 0$. Let us determine now that constant level. Solving the first two equations of (100) for λ_2/λ_3 delivers:

$$\frac{\lambda_2}{\lambda_3} = -\frac{\pi'\sigma - (\pi - k_h x_3/x_2)\sigma'}{\mu'\sigma - \mu\sigma'} \tag{102}$$

From $k_h = 0$ it follows that $\lambda_2(t)$ and $\lambda_3(t)$ are constant for all t, so from boundary conditions (37) we obtain:

$$\lambda_2(t) = \lambda_2(t_f) = 0 \tag{103}$$

$$\lambda_3(t) = \lambda_3(t_f) = -1 \tag{104}$$

As a consequence, equation (102) reduces to:

$$\pi'\sigma - \pi\sigma' = 0 \tag{105}$$

or in other words the singular control extremizes the *product yield*:

$$\frac{d}{dC_s}(\frac{\pi}{\sigma}) = 0 \tag{106}$$

which completes the proof.

□

Let us first formulate some remarks. First of all, the specific rates σ, μ and π are required to be *smooth* functions of C_s, in order to ensure the existence and continuity of at least the first two derivatives with respect to C_s, thus enabling the calculation of $u_{sing}(t)$ with equation (98). Note that the singular control is *linear* in the hydrolysis k_h:

$$u_{sing}(t) = \frac{s_F\sigma X}{s_F - C_s} + k_h \frac{s_F G\lambda_3(\pi' x_2 - \mu' x_3)}{x_2(s_F - C_s)(\lambda_1\sigma'' - \lambda_2\mu'' - \lambda_3\pi'')} \tag{107}$$

It follows from the above theorem that the condition $k_h = 0$ is also necessary and sufficient to obtain the complete optimal control for a given S_0 as a *closed-loop* solution : clearly the switching from *batch* to *singular* control is then dictated by the condition $C_s = C_s^*$, C_s^* denoting the value of C_s for which π/σ has its optimum. Remark also that there is, for the kinetics σ, μ and π known in the literature for the penicillin fermentation, only one extremal value for the yield π/σ which is indeed a *maximum*. At this point we could generalize the above results to performance indices of the form:

$$J(u) = g(\mathrm{x}(t_f)) \tag{108}$$

Again, the singular control keeps the substrate concentration at a constant level *if and only if* $k_h = 0$, where that constant level must satisfy the relation:

$$\lambda_2(t_f)(\mu'\sigma - \mu\sigma') + \lambda_3(t_f)(\pi'\sigma - \pi\sigma') = 0 \tag{109}$$

Let us now concentrate a bit more on the somewhat artificial condition $m_s > 0$. In particular, what happens if $m_s = 0$? From the above proof we know that in fact only the case where *both* m_s *and* k_h *equal zero* needs additional justification.

We have :

$$\sigma(C_s) = \frac{\mu(C_s)}{Y_{x/s}} + \frac{\pi(C_s)}{Y_{p/s}} \tag{110}$$

where two specific rates are to be given. It is not quite difficult to show now that the dimension of the state can be reduced by one[16]. Using the system-equations (74) the above equation can be written as follows:

$$udt = dS + \frac{1}{Y_{x/s}}dX + \frac{1}{Y_{p/s}}dP \tag{111}$$

Integrating from $t = t_0$ delivers:

$$s_F(G(t) - G_0) = S(t) - S_0 + \frac{1}{Y_{x/s}}(X(t) - X_0) + \frac{1}{Y_{p/s}}(P(t) - P_0) \tag{112}$$

With:

$$G_0 = G_* + S_0/s_F \qquad P_0 = 0 \tag{113}$$

this leads to:

$$P(t) = Y_{p/s}(s_F(G(t) - G_*) - S(t) - \frac{1}{Y_{x/s}}(X(t) - X_0)) \tag{114}$$

We conclude that we can drop the differential equation for P, $P(t)$ being determined for all t by the above *algebraic* equation. Noting that the total amount of substrate is limited:

$$S_0 + \int_{t_0}^{t_f} u dt = \alpha \tag{115}$$

or, using the last state–equation:

$$s_F(G_f - G_*) = \alpha \tag{116}$$

we obtain on $t = t_f$:

$$P(t_f) = Y_{p/s}(\alpha + X_0/Y_{x/s}) - Y_{p/s}(S(t_f) + X(t_f)/Y_{x/s}) \tag{117}$$

If we want to maximize the final amount of product $P(t_f)$, we conclude that this is equivalent to minimizing the following performance measure:

$$J(u) = S(t_f) + X(t_f)/Y_{x/s} \tag{118}$$

Note that this is clearly in contradiction with the result of Duvivier and Sevely[16], who claimed that the problem would become a *minimal time* problem!

For reasons of compatibility with the above notations, we shall denote the costate vector as:

$$\lambda(t) \triangleq \begin{pmatrix} \lambda_1(t) \\ \lambda_2(t) \\ \lambda_4(t) \end{pmatrix} \tag{119}$$

with boundary conditions:

$$\lambda(t_f) = \frac{\partial g}{\partial \mathrm{x}} = \begin{pmatrix} 1 \\ 1/Y_{x/s} \\ - \end{pmatrix} \tag{120}$$

The Hamiltonian H is given by equation (82), where the functions ϕ and ψ reduce to :

$$\phi = (-\lambda_1\sigma + \lambda_2\mu)x_2 \qquad \psi = \lambda_1 + \lambda_4/s_F \tag{121}$$

The adjoint equations become:

$$\dot{\lambda}_1 = (\lambda_1\sigma' - \lambda_2\mu')x_2/x_4 \tag{122}$$

$$\dot{\lambda}_2 = \lambda_1\sigma - \lambda_2\mu \tag{123}$$

$$\dot{\lambda}_4 = -(\lambda_1\sigma' - \lambda_2\mu')x_1x_2/x_4^2 \tag{124}$$

On the singular interval, we obtain :

$$\lambda_1 + \lambda_4/s_F = 0 \tag{125}$$

$$\lambda_1\sigma - \lambda_2\mu = 0 \tag{126}$$

$$\lambda_1\sigma' - \lambda_2\mu' = 0 \tag{127}$$

which again results in a *constant* costate–vector on the singular interval. We also have:

$$\lambda_2(t) = \lambda_2(t_f) = \frac{1}{Y_{x/s}} \tag{128}$$

For the above system to have a non–trivial solution $\lambda(t)$, it is *necessary and sufficient* that:

$$\sigma'\mu - \sigma\mu' = 0 \tag{129}$$

or, in other words:

$$\frac{d}{dC_s}(\frac{\sigma}{\mu}) = 0 \tag{130}$$

or, using balance (81):

$$\frac{d}{dC_s}(\frac{\pi}{\sigma}) = 0 \tag{131}$$

which determines the *constant* value of C_s during singular control. Note that $d^2\psi/dt^2 = 0$ leads to:

$$(\lambda_1\sigma'' - \lambda_2\mu'')\dot{C}_s = 0 \tag{132}$$

Clearly, $\lambda_1\sigma'' - \lambda_2\mu''$ cannot be zero, so we obtain indeed:

$$\dot{C}_s = 0 \tag{133}$$

resulting in

$$u_{sing}(t) = \frac{s_F\sigma X}{s_F - C_s} \tag{134}$$

The terminal time t_f for this case is obtained as follows. During the last batch–phase, we have $u = 0$, so from (82) we obtain:

$$\phi(t_f) = 0 \tag{135}$$

Using boundary conditions (37) this results in:

$$-\sigma(t_f) + \mu(t_f)/Y_{x/s} = 0 \tag{136}$$

or using balance (81):

$$\pi(t_f) = 0 \tag{137}$$

This is equivalent with:

$$\frac{dP}{dt} = 0 \tag{138}$$

as we might expect on *physical* grounds. Note that for specific production rate (79) this means that:

$$C_s(t_f) = 0 \tag{139}$$

Again we can easily generalize these results to a more general performance measure (108), wherein $P(t_f)$ has to be replaced by expression (117). Note that the specific expression for $g(\mathrm{x}(t_f))$ does *not* influence the constant level of C_s during singular control. It only determines the final time t_f through condition (135).

We now summarize these results in a more general theorem.

Theorem 2 *Consider the given system* (74) *with performance index* $J(u) = g(\mathrm{x}(t_f))$, *subject to the specified constraints and with* t_f *free. Suppose that* σ, μ *and* π *are functions of* C_s *only with continuous second derivatives.*
Then during singular control the substrate concentration remains constant if and only if the hydrolysis $k_h = 0$.
If $m_s > 0$, *the substrate concentration satisfies :*

$$\frac{\partial g}{\partial x_2}(t_f)(\mu'\sigma - \mu\sigma') + \frac{\partial g}{\partial x_3}(t_f)(\pi'\sigma - \pi\sigma') = 0$$

If $m_s = 0$, *the substrate concentration satisfies :*

$$\pi'\sigma - \pi\sigma' = 0$$

and is independent of the specific form of $g(\mathrm{x})$. *In both cases, the Optimal Control is obtained in closed–loop for a given* S_0.

For the model handled in the text, the specific rates are given by (78), (79) and (81). We already know that these represent a sequence of completely smooth models, that converge to the *original* piecewise smooth model as $B \to 0$. For $B = 0$, standard optimal control theory does *not* hold. However, the above theorems apply to every B in $0 < B \leq \mu_{crit}$. Following the *conjecture* of Section 2, we know that the Optimal Control for $B = 0$ is the limit for $B \to 0$ of the sequence of Optimal Controls for B within $0 < B \leq \mu_{crit}$. We then prove the following theorem :

Theorem 3 *Consider the system* (74) *with performance index* $J(u) = -P(t_f)$, *subject to the specified constraints and with* t_f *free. The piecewise smooth specific rates are given by* (5), (6) *and* (7). *Then during singular control the substrate concentration remains constant if and only if the hydrolysis* $k_h = 0$, *and is determined by the equation:*

$$\mu = \mu_{crit}$$

This constant value maximizes the yield π/σ.

PROOF

In the following, a prime denotes derivation with respect to substrate concentration. Consider B in $0 < B \leq \mu_{crit}$. In Section 2, we have shown that the specific rates (78), (79) and (81) are functions of C_s only. Following Theorem 1, we know that on the singular interval C_s remains constant if and only if $k_h = 0$. C_s satisfies :

$$\pi'\sigma - \sigma'\pi = 0 \tag{140}$$

We have:

$$\frac{d\pi}{dC_s} = \frac{d\pi}{d\mu}\frac{d\mu}{dC_s} \tag{141}$$

Noting that:

$$\frac{d\mu}{dC_s} = Y_{x/s}\left(\frac{d\sigma}{dC_s} - \frac{1}{Y_{p/s}}\frac{d\pi}{dC_s}\right) \tag{142}$$

we obtain an equation in π', which can be written as follows:

$$\pi' = F(\mu, B)\sigma' \tag{143}$$

where

$$F(\mu, B) \triangleq \frac{Q_{p,max}Y_{x/s}[1 - (\mu - \mu_{crit} + 2B)/R(\mu, B)]/[2(\mu_{crit} - B)]}{1 + Q_{p,max}Y_{x/s}[1 - (\mu - \mu_{crit} + 2B)/R(\mu, B)]/[2(\mu_{crit} - B)Y_{p/s}]} \tag{144}$$

$$R(\mu, B) \triangleq \sqrt{(\mu + \mu_{crit})^2 - 4(\mu_{crit} - B)\mu} \tag{145}$$

We obtain, using (140) with $\sigma' \neq 0$:

$$F(\mu, B)\left(\frac{\mu}{Y_{x/s}} + m_s + \frac{\pi}{Y_{p/s}}\right) = \pi \tag{146}$$

Considering the limit for $B \to 0$ on both sides of the above equation, we obtain:

$$Y_{x/s}[\mid \mu - \mu_{crit} \mid -(\mu - \mu_{crit})][\frac{\mu}{Y_{x/s}} + m_s + \frac{Q_{p,max}}{2Y_{p/s}\mu_{crit}}(\mu + \mu_{crit} - \mid \mu - \mu_{crit} \mid)] =$$

$$[\mu + \mu_{crit} - \mid \mu - \mu_{crit} \mid][\mid \mu - \mu_{crit} \mid + \frac{Y_{x/s}Q_{p,max}}{2Y_{p/s}\mu_{crit}}(\mid \mu - \mu_{crit} \mid -(\mu - \mu_{crit}))]$$

Solving for μ obviously leads to:

$$\mu = \mu_{crit} \tag{147}$$

Using equation (81), the substrate concentration during singular control is:

$$C_{s,sing} \triangleq C_{s,crit} = K_s\frac{\mu_{crit}/Y_{x/s} + m_s + Q_{p,max}/Y_{p/s}}{Q_{s,max} - (\mu_{crit}/Y_{x/s} + m_s + Q_{p,max}/Y_{p/s})} \tag{148}$$

Figure 14 shows values of π/σ as a function of C_s, for different values of B. We conclude that for $B = 0$, π/σ takes on its maximum value for $C_s = C_{s,crit}$.

□

In Figure 15 we show the optimal switching values for μ and the corresponding value C_s for different values of B, with $k_h = 0$. Remark the convergence to $\mu \to \mu_{crit}$, $C_s \to C_{s,crit}$ as $B \to 0$.

Figure 14 *π/σ as a function of C_s for some values of B*
Figure 15 *Optimal switching values for μ and C_s as a function of B with $k_h = 0$*

Remark also that setting $B = 10^{-11}$ in (79) is a very accurate approximation of the original kinetics (6), as the last figures show.

In general, hydrolysis $k_h \neq 0$, so we do not know the switching time t_2 in *closed–loop* form, i. e. as a function of state–variables only. However, the above theorems give a good initial guess for t_2 if k_h is sufficiently small. They also indicate that during singular control, the substrate concentration shall vary in time. Of course for small k_h, this time dependence shall be small also, as is illustrated by the simulation results.

Acknowledgements

The previous text presents research results partially of the Belgian National incentive-program on fundamental research in Life Sciences initiated by the Belgian State — Prime Minister's Office — Science Policy Programming. The scientific responsability is assumed by its authors.

References

1 Heijnen, J. J., J. A. Roels and A. H. Stouthamer, 'Application of Balancing Methods in Modeling the Penicillin Fermentation', *Biotechnol. Bioeng.*, 21, 2175–2201 (1979)

2 Bajpai, R. K. and M. Reuß, 'A Mechanistic Model for Penicillin Production', *J. Chem. Tech. Biotechnol.*, 30, 332-344 (1980)

3 Bajpai, R. K. and M. Reuß, 'Evaluation of Feeding Strategies in Carbon–regulated Secondary Metabolite Production through Mathematical Modelling', *Biotechnol. Bioeng.*, 23, 717–738 (1981)

4 Lim, H. C., Y. J. Tayeb, J. M. Modak and P. Bonte, 'Computational algorithms for Optimal Feed Rates for a Class of Fed–Batch Fermentation: Numerical Results for Penicillin and Cell Mass Production', *Biotechnol. Bioeng.*, 28, 1408–1420 (1986)

5 Bonte, G., J. F. Van Impe and J. A. Spriet, 'Feeding Strategy Optimization of the Penicillin Fed–Batch Fermentation using a Mathematical Model', *Med. Fac. Landbouww. Rijksuniv. Gent*, 54 (4a), 1215–1224 (1989)

6 Van Impe, J. F., B. M. Nicolaï, P. A. Vanrolleghem, J. A. Spriet and J. Vandewalle, 'Optimal Control of the Penicillin G Fed–Batch Fermentation : An Analysis of the Model of Bajpai and Reuß', *ESAT–SISTA Report*, Department of Electrical Engineering, K. U. Leuven (1990)

7 Van Impe, J. F., B. M. Nicolaï, P. A. Vanrolleghem, J. A. Spriet and J. Vandewalle, 'Optimal Control of the Penicillin G Fed–Batch Fermentation : Evaluation of the Model of Heijnen et al. and the Model of Bajpai and Reuß for Control Purposes', *ESAT–SISTA Report*, Department of Electrical Engineering, K. U. Leuven (1990)

8 Roels, J. A., *Energetics and Kinetics in Biotechnology*, Chapter 9, Elsevier Biomedical Press, Amsterdam – New York – Oxford, 1983

9 Athans, M. and P. L. Falb, *Optimal Control*, McGraw–Hill, New York, 1966

10 Pontryagin, L. S., V. G. Boltyanskii, R. V. Gamkrelidze and E. F. Mishchenko, *The Mathematical Theory of Optimal Processes*, Wiley–Interscience, New York, 1962

11 Ryu, D. Y. and A. E. Humphrey, *The Practice of Biotechnology : Penicillins*, in *Comprehensive Biotechnology* Volume 3, Ed. M. Moo-Young, Pergamon Press, Oxford, 1985

12 Bonte, G., 'Influence of Structural Differences in Fed-Batch Models for Penicillin Fermentation on Product Optimization', *M.Sc. thesis* (in Dutch), K. U. Leuven (1989)

13 Dochain, D. and G. Bastin, 'Adaptive Identification and Control Algorithms for non linear Bacterial Growth Systems', *Automatica*, Special Issue on Adaptive Control, 20, 621-634 (1984)

14 Bryson, A. E. Jr. and Y.-C. Ho, *Applied Optimal Control*, Hemisphere, Washington - New York - London, 1975

15 Modak, J. M., H. C. Lim and Y. J. Tayeb, 'General Characteristics of Optimal Feed Rate Profiles for Various Fed-Batch Fermentation Processes', *Biotechnol. Bioeng.*, 28, 1396-1407 (1986)

16 Duvivier, E. and Y. Sevely, 'Simulation de la commande en temps minimal d'un procédé de fermentation en semi-continu : Transformation de Kelley et Programmation Dynamique', *R.A.I.R.O*, 22, 363-380 (1988)

List of Figures

Figure 1a *The specific rates σ and μ as functions of C_s*

Figure 1b *The specific rate π as a function of C_s*

Figure 2 *Dabes-kinetics $\pi(\mu)$ for some values of parameter B*

Figure 3 *Constant glucose feed rate and corresponding cell, glucose, product, μ and π profiles*

Figure 4 *Extremal values for $P(t_f)$, t_2 and t_f as functions of S_0 for $B = 10^{-11}$*

Figure 5 *Optimal glucose feed rate and corresponding cell, glucose, product, π and μ profiles for $B = 10^{-11}$*

Figure 6 *Extremal values for $P(t_f)$, t_2 and t_f as functions of S_0 for $B = 10^{-2}$*

Figure 7 *Optimal glucose feed rate and corresponding cell, glucose, product, π and μ profiles for $B = 10^{-2}$*

Figure 8 *Optimal production P_f as a function of B*

Figure 9 *Suboptimal glucose feed rate and corresponding cell, glucose, product, π and μ profiles for $B = 10^{-11}$*

Figure 10 *Suboptimal and Optimal glucose feed rate for $B = 10^{-11}$*

Figure 11 *Suboptimal glucose feed rate and corresponding cell, glucose, product, π and μ profiles for $B = 10^{-2}$ and $\mu_{switch} = \mu_{crit}$*

Figure 12 *Suboptimal glucose feed rate and corresponding cell, glucose, product, π and μ profiles for $B = 10^{-2}$ and μ_{switch} free*

Figure 13 *Suboptimal and Optimal glucose feed rate for $B = 10^{-2}$*

Figure 14 *π/σ as a function of C_s for some values of B*

Figure 15 *Optimal switching values for μ and C_s as a function of B with $k_h = 0$*

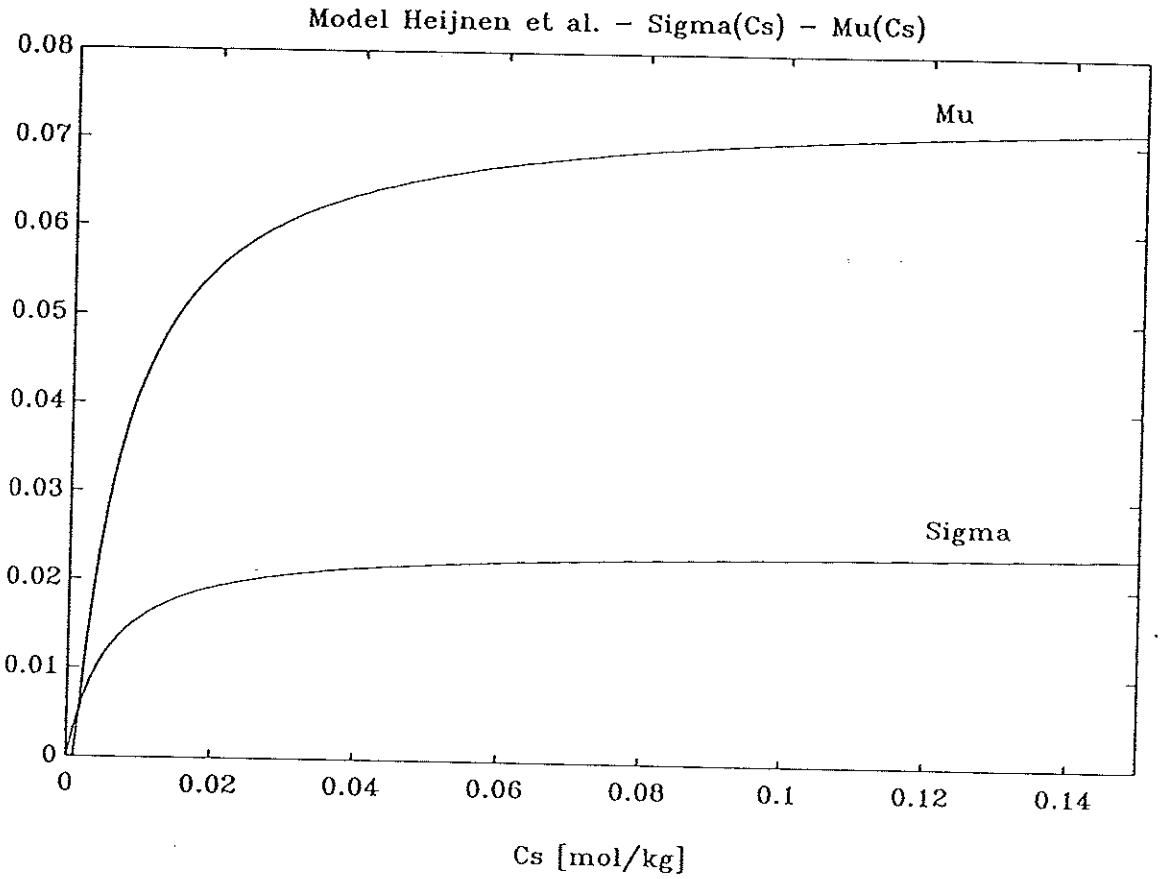

Figure 1a *The specific rates σ and μ as functions of C_s*

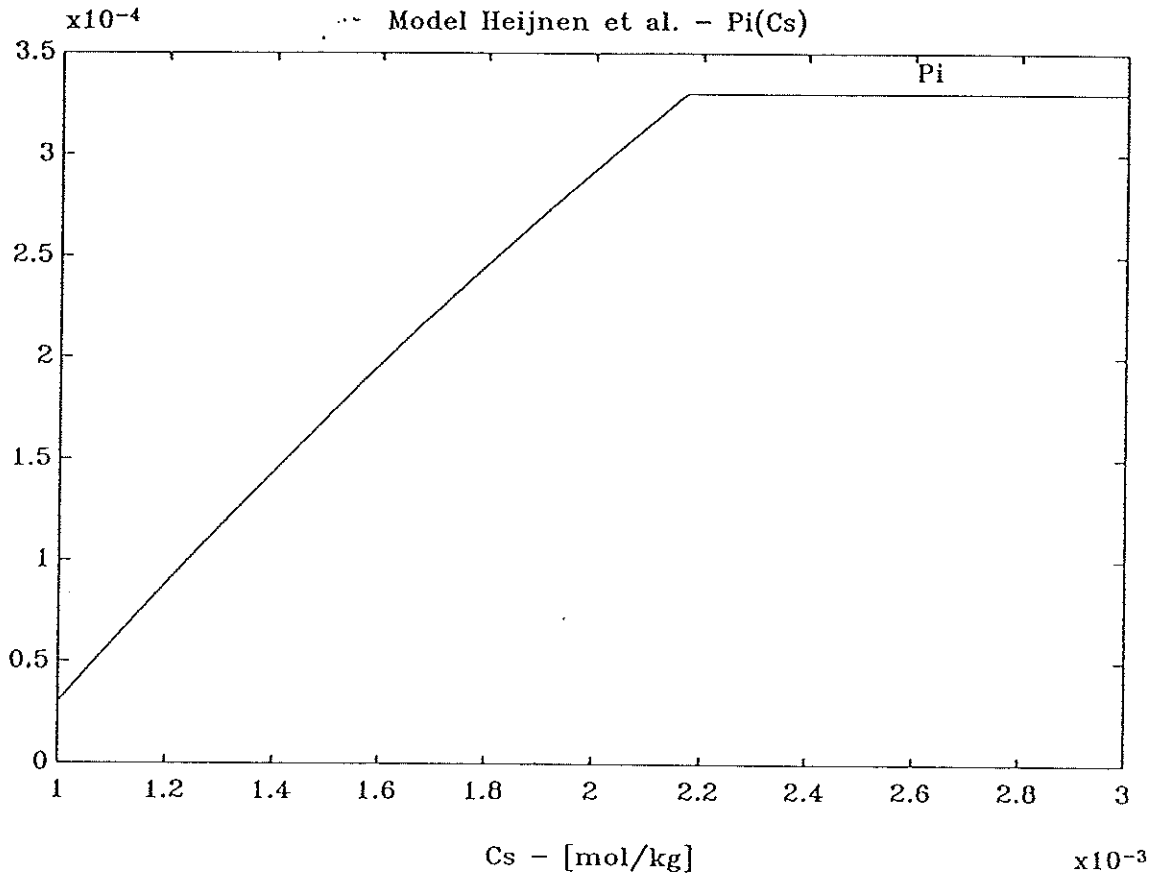

Figure 1b *The specific rate π as a function of C_s*

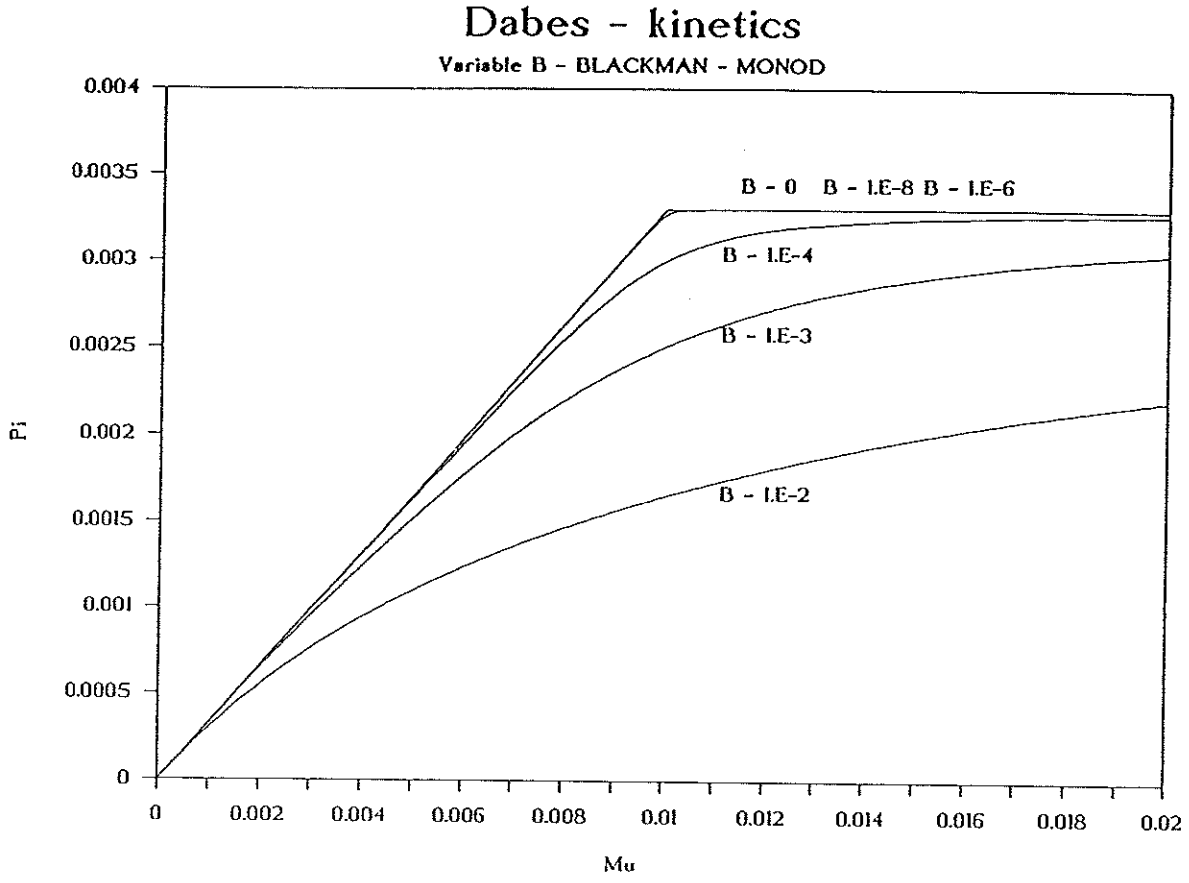

Figure 2 *Dabes-kinetics $\pi(\mu)$ for some values of parameter B*

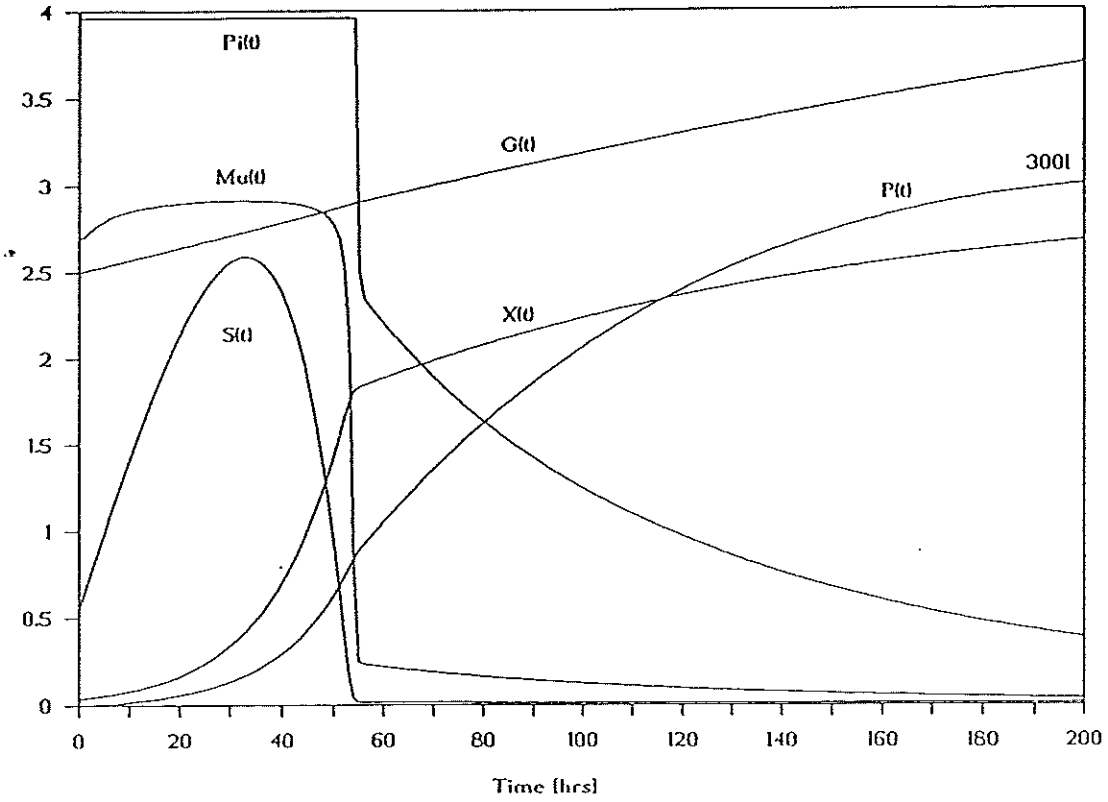

Scaling $S(t)/10^{1}$, $X(t)/10^{5}$, $P(t)/10^{3}$, $G(t)/4\ 10^{1}$, $\mu(t) * 40$, $\pi(t) * 12\ 10^{3}$

Figure 3 *Constant glucose feed rate and corresponding cell, glucose, product, μ and π profiles*

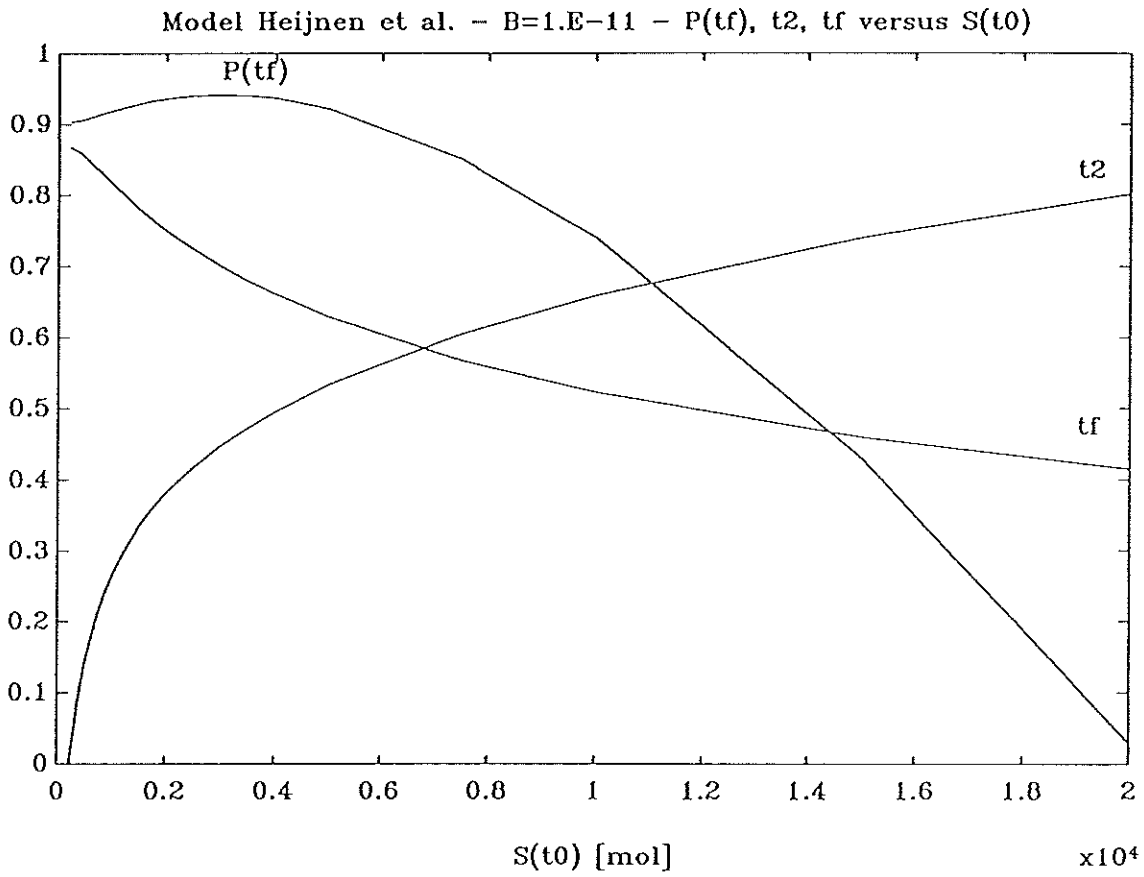

Scaling $t_2/50$, $t_f/500$, $(P(t_f) - 8150)/180$

Figure 4 *Extremal values for* $P(t_f)$, t_2 *and* t_f *as functions of* S_0 *for* $B = 10^{-11}$

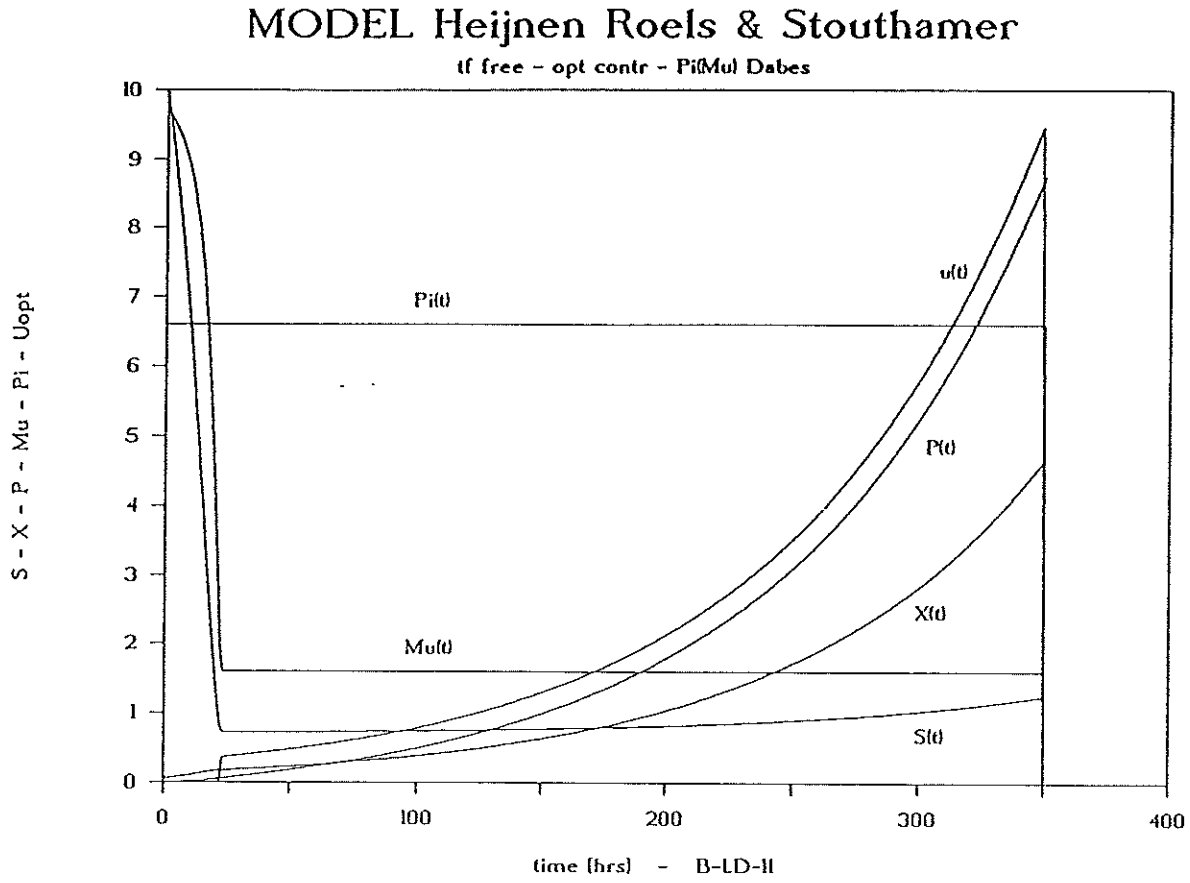

Scaling $S(t)/300$, $X(t)/66\ 10^{3}$, $P(t)/950$, $u(t)/220$, $\mu(t) * 160$, $\pi(t) * 2\ 10^{4}$

Figure 5 *Optimal glucose feed rate and corresponding cell, glucose, product,* π *and* μ *profiles for* $B = 10^{-11}$

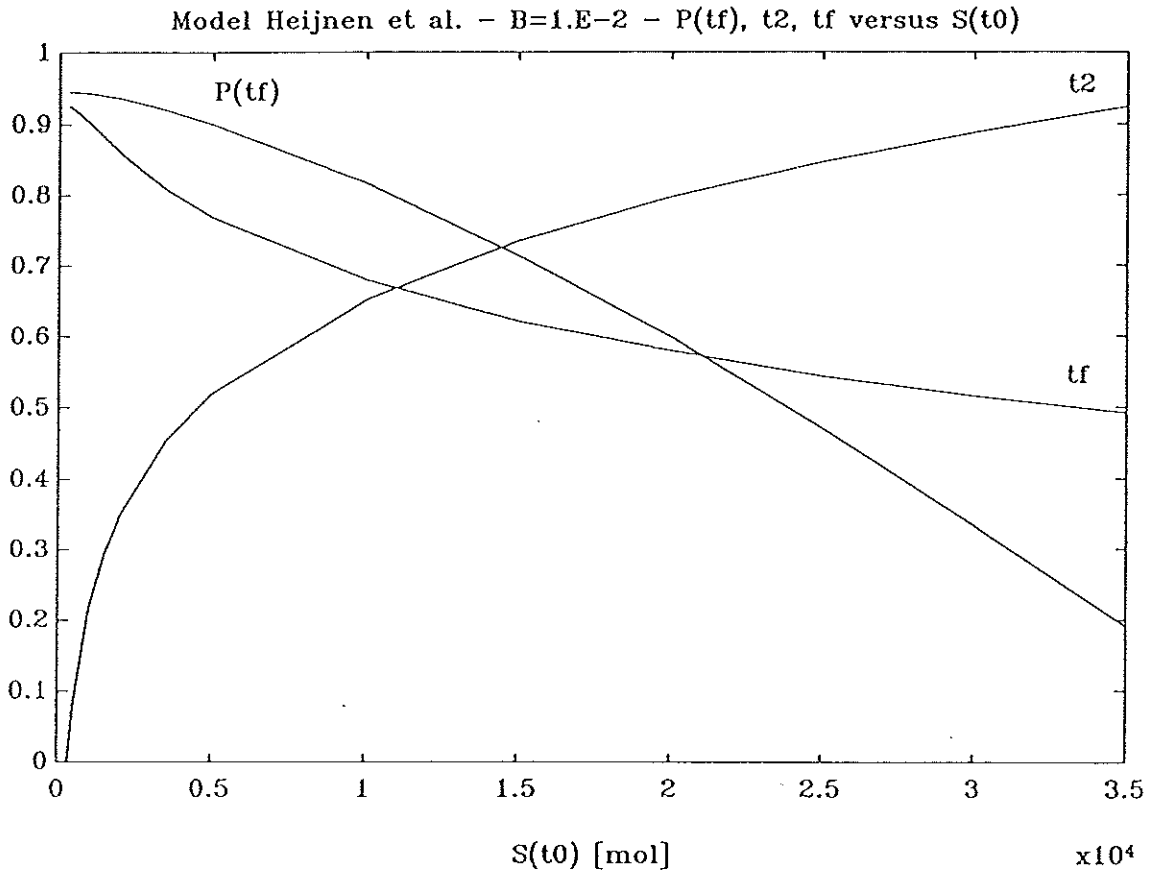

Scaling $t_2/50$, $t_f/300$, $(P(t_f) - 4300)/280$

Figure 6 *Extremal values for* $P(t_f)$, t_2 *and* t_f *as functions of* S_0 *for* $B = 10^{-2}$

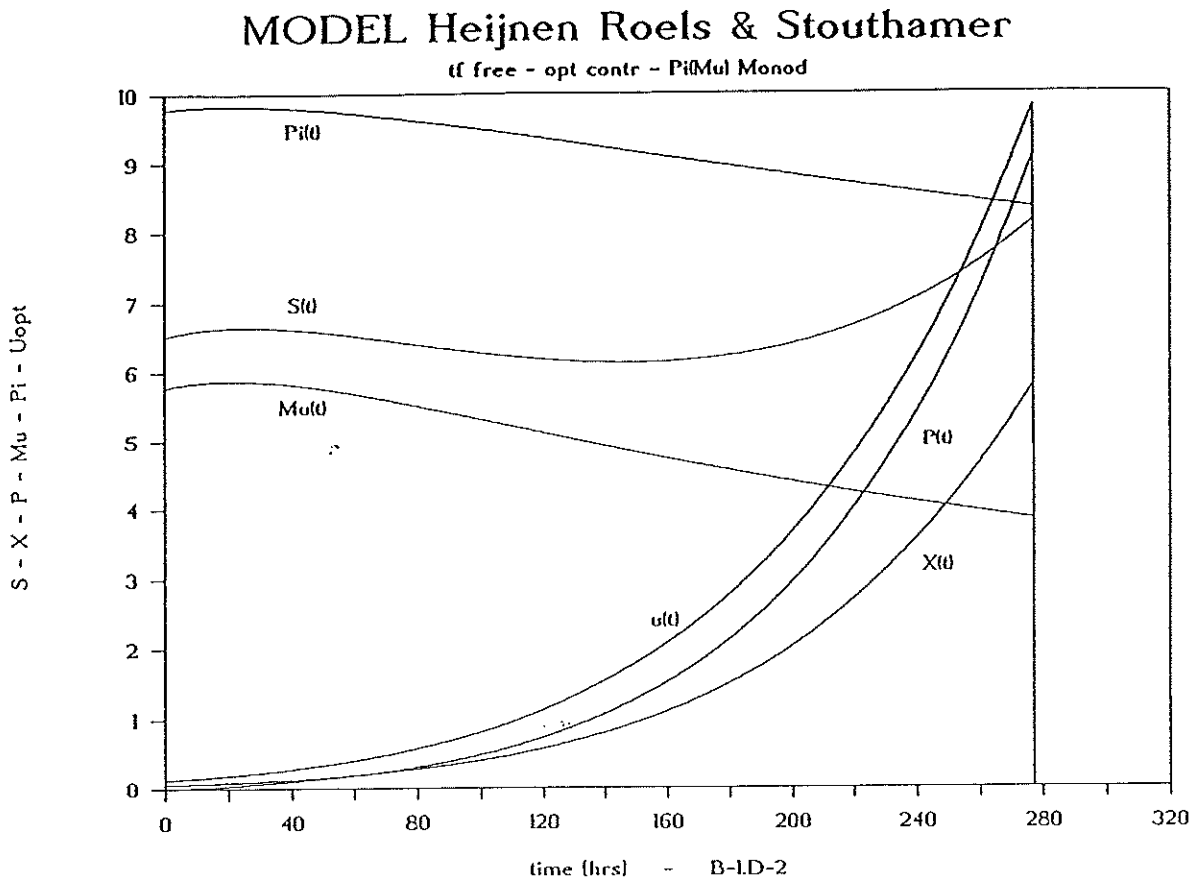

Scaling $S(t)/50$, $X(t)/66\ 10^{3}$, $P(t)/500$, $u(t)/285$, $\mu(t) * 300$, $\pi(t) * 45\ 10^{3}$

Figure 7 *Optimal glucose feed rate and corresponding cell, glucose, product, π and μ profiles for $B = 10^{-2}$*

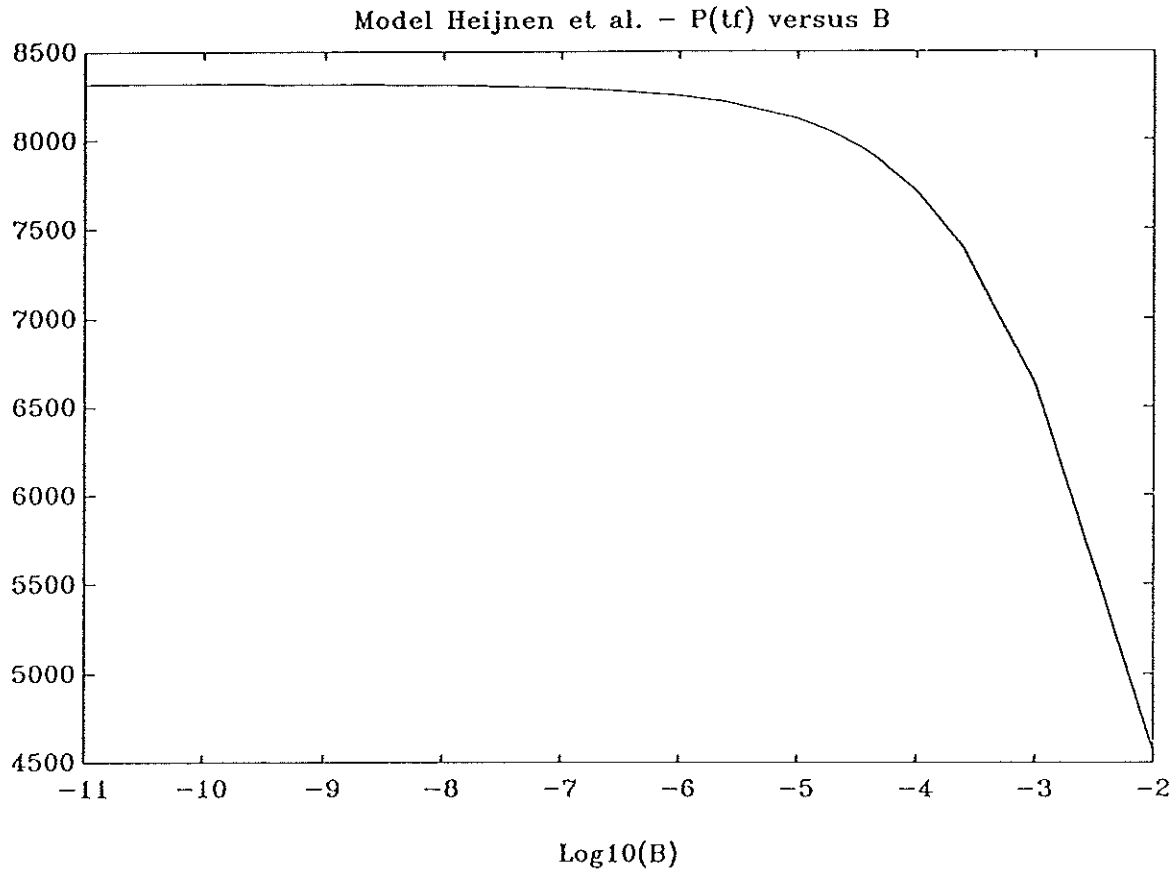

Figure 8 *Optimal production P_f as a function of B*

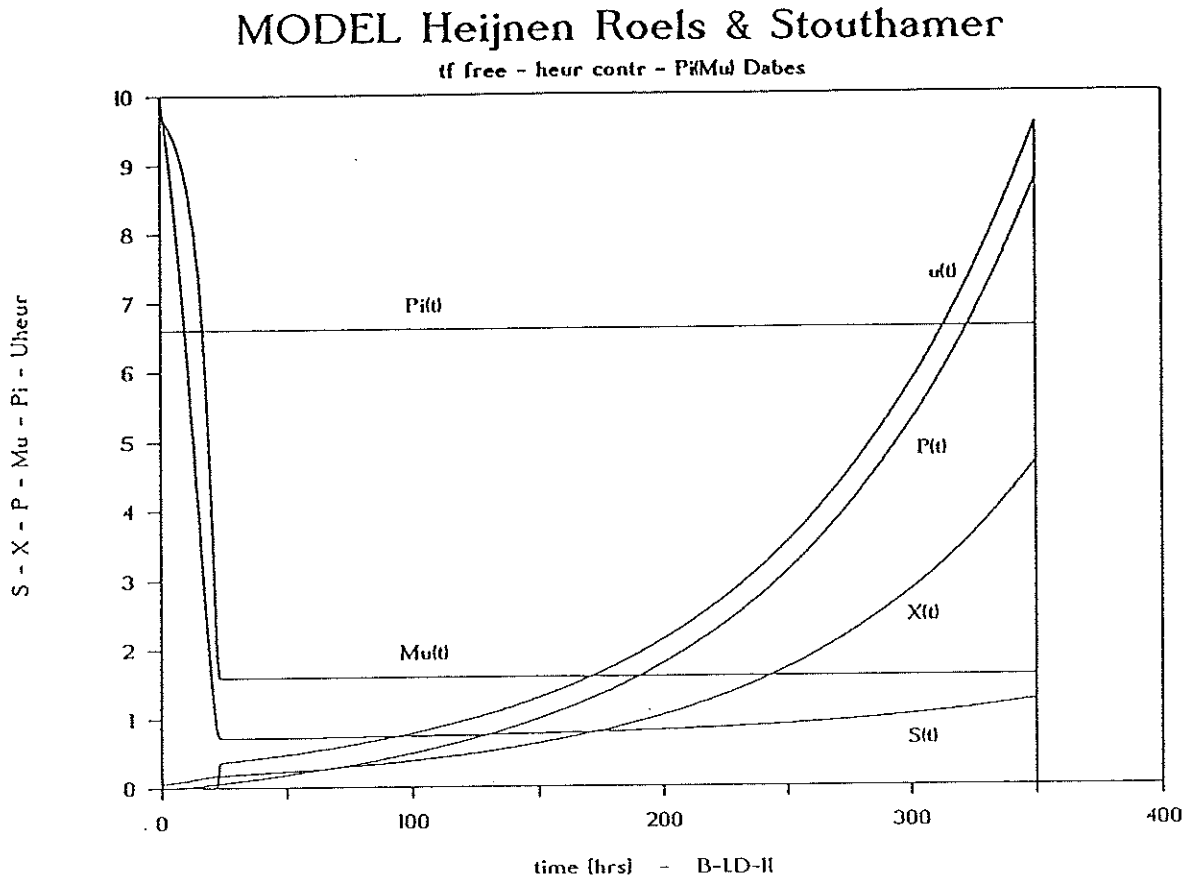

Scaling $S(t)/300$, $X(t)/66\ 10^3$, $P(t)/950$, $u(t)/220$, $\mu(t) * 160$, $\pi(t) * 2\ 10^4$

Figure 9 *Suboptimal glucose feed rate and corresponding cell, glucose, product, π and μ profiles for $B = 10^{-11}$*

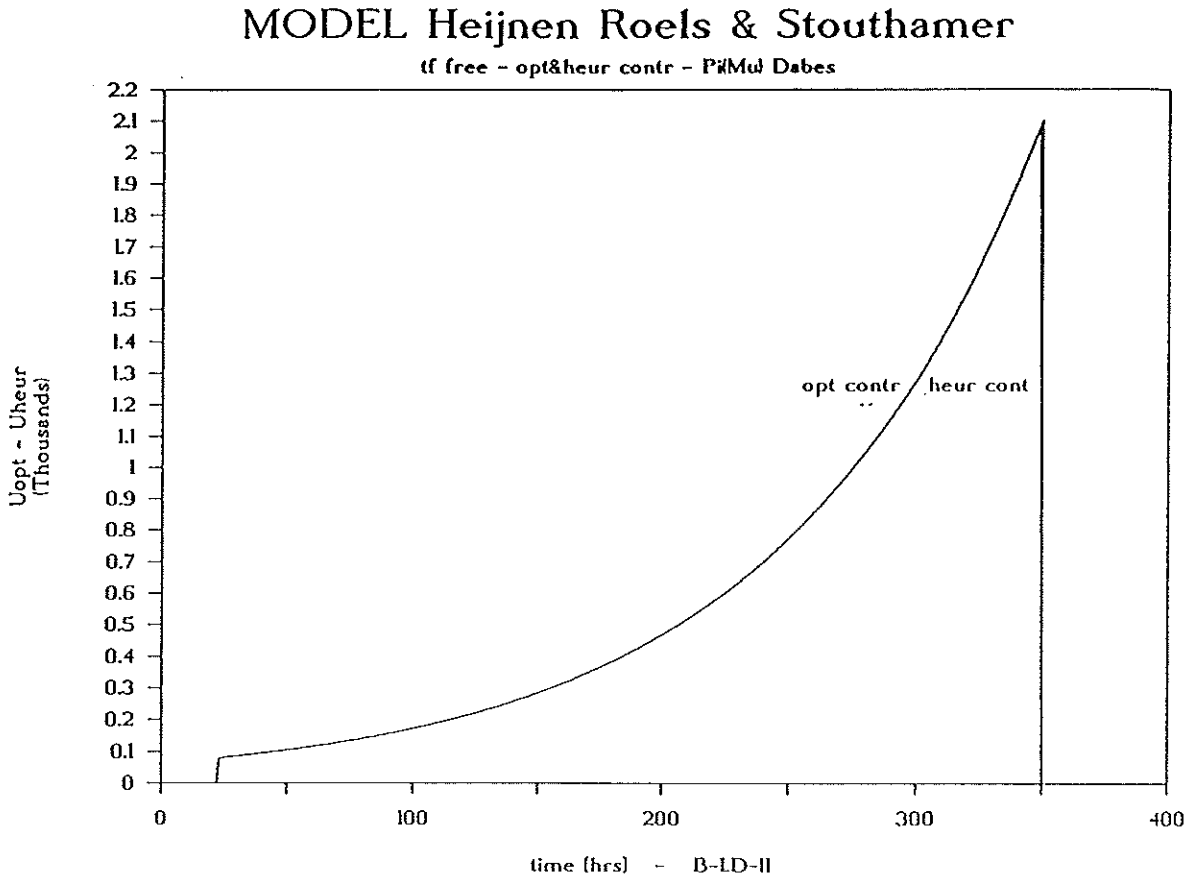

Figure 10 *Suboptimal and Optimal glucose feed rate for* $B = 10^{-11}$

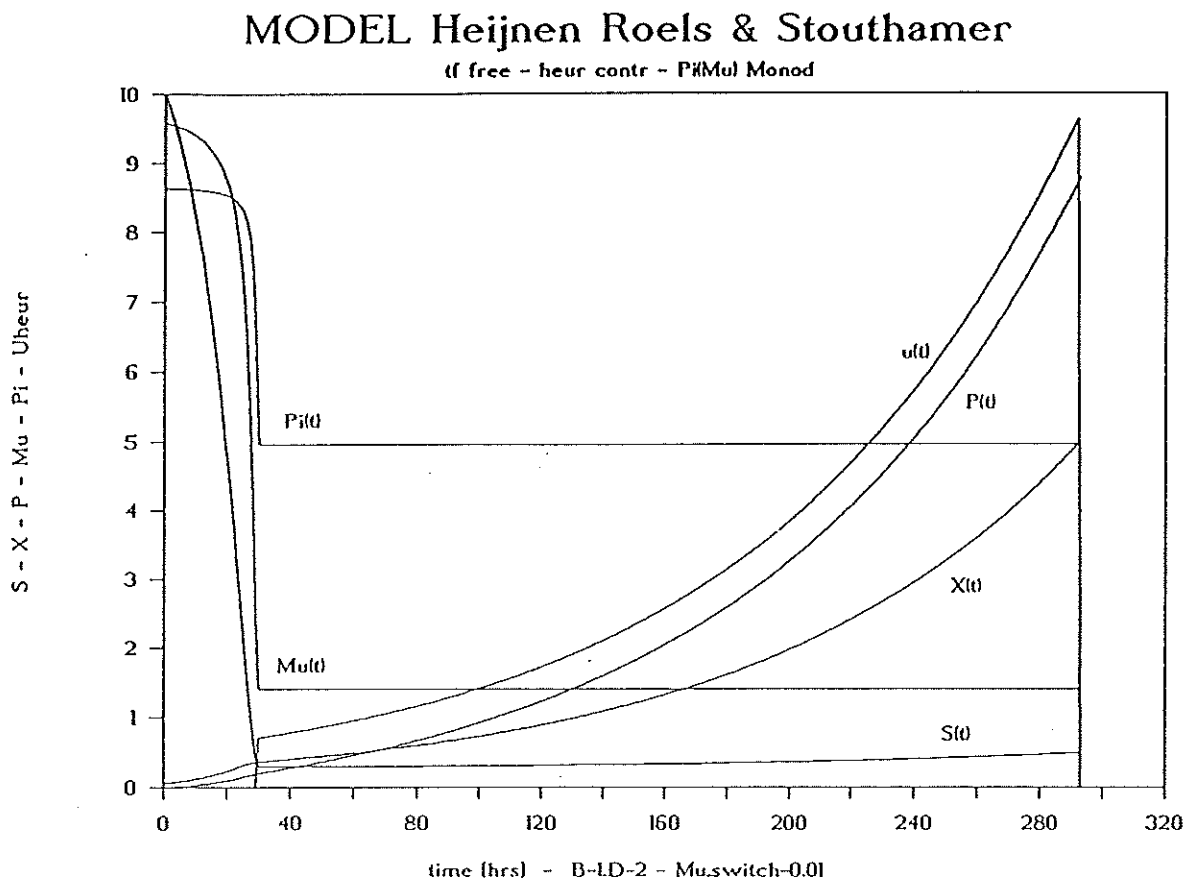

Scaling $S(t)/700$, $X(t)/66\ 10^{3}$, $P(t)/500$, $u(t)/220$, $\mu(t) * 140$, $\pi(t) * 3\ 10^{4}$

Figure 11 *Suboptimal glucose feed rate and corresponding cell, glucose, product, π and μ profiles for $B = 10^{-2}$ and $\mu_{switch} = \mu_{crit}$*

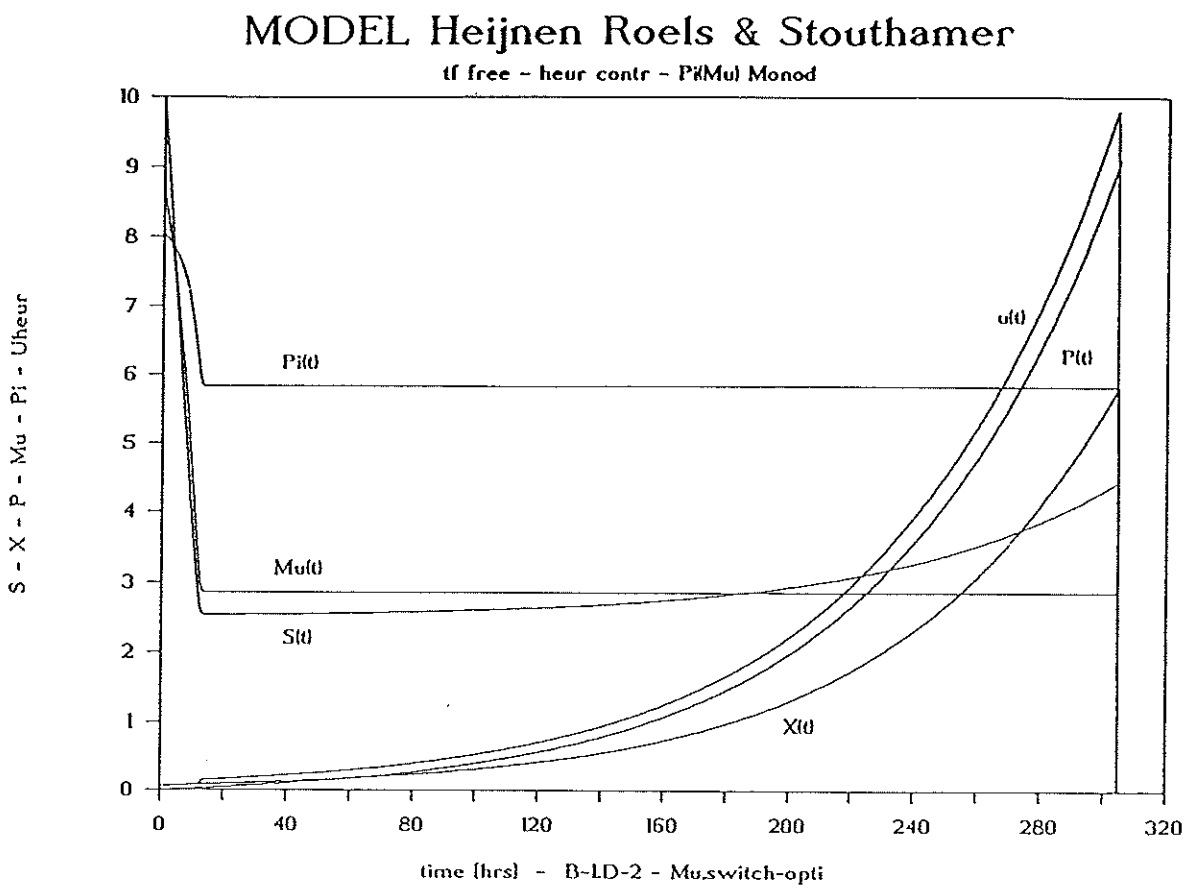

Scaling $S(t)/100$, $X(t)/66\ 10^{3}$, $P(t)/500$, $u(t)/300$, $\mu(t) * 200$, $\pi(t) * 3\ 10^{4}$

Figure 12 *Suboptimal glucose feed rate and corresponding cell, glucose, product, π and μ profiles for $B = 10^{-2}$ and μ_{switch} free*

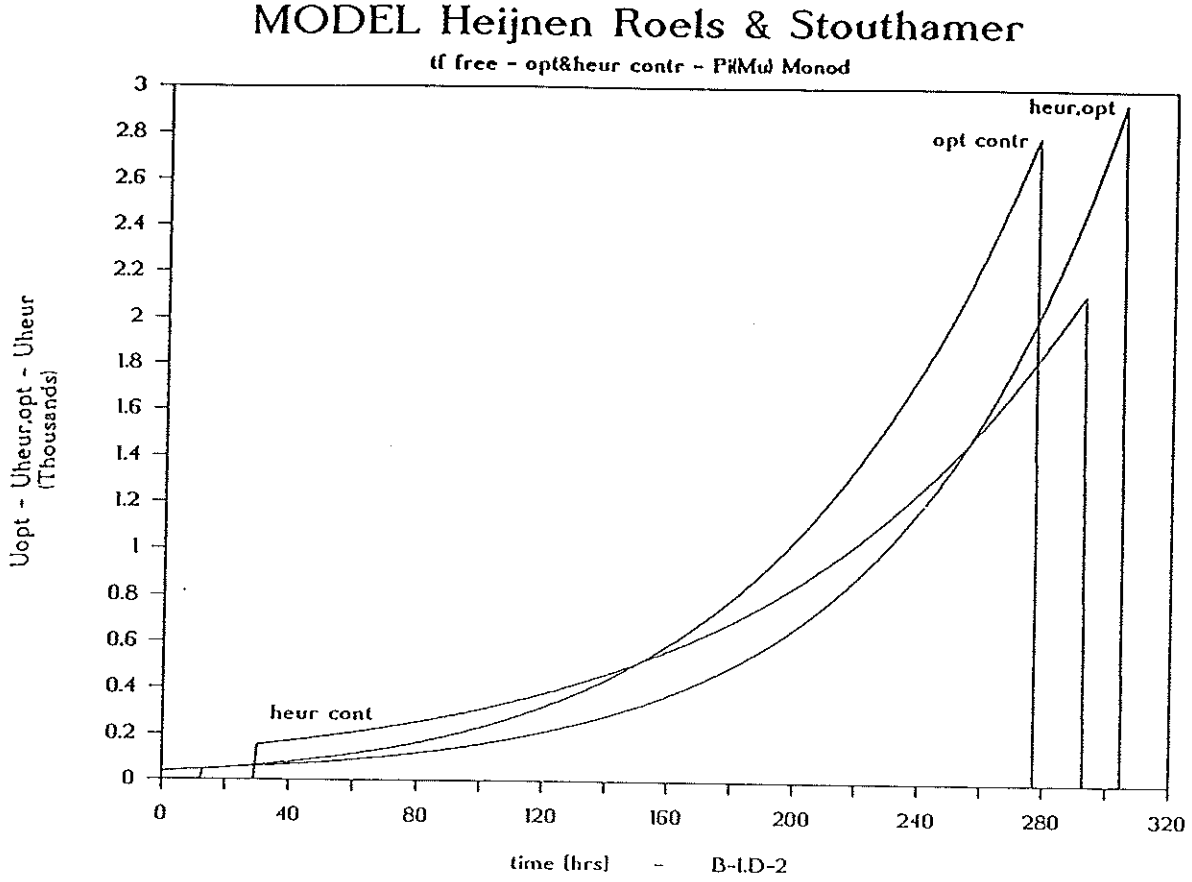

Legend *opt contr* ≡ optimal control - *heur cont* ≡ heuristic control with $\mu_{switch} = \mu_{crit}$
heur,opt ≡ heuristic control with μ_{switch} free

Figure 13 *Suboptimal and Optimal glucose feed rate for* $B = 10^{-2}$

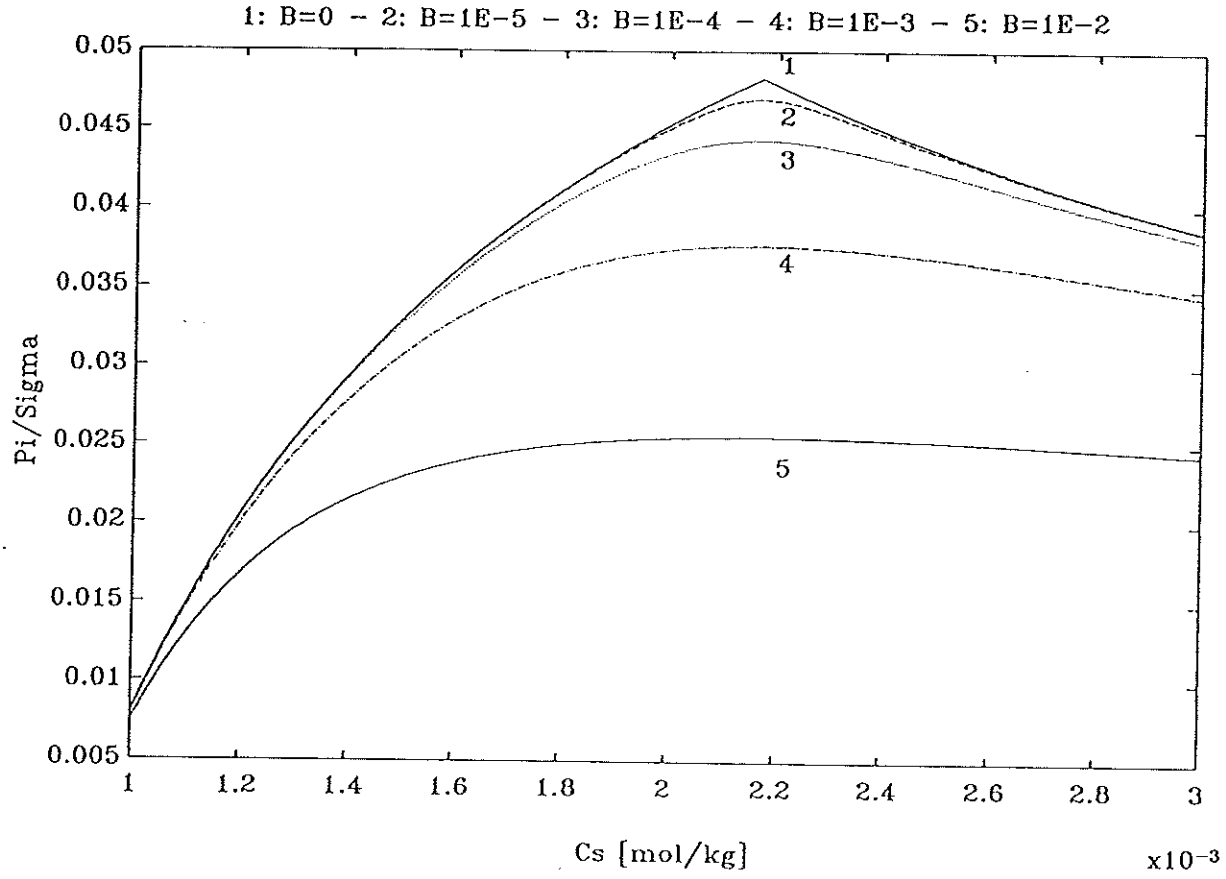

Figure 14 *π/σ as a function of C_s for some values of B*

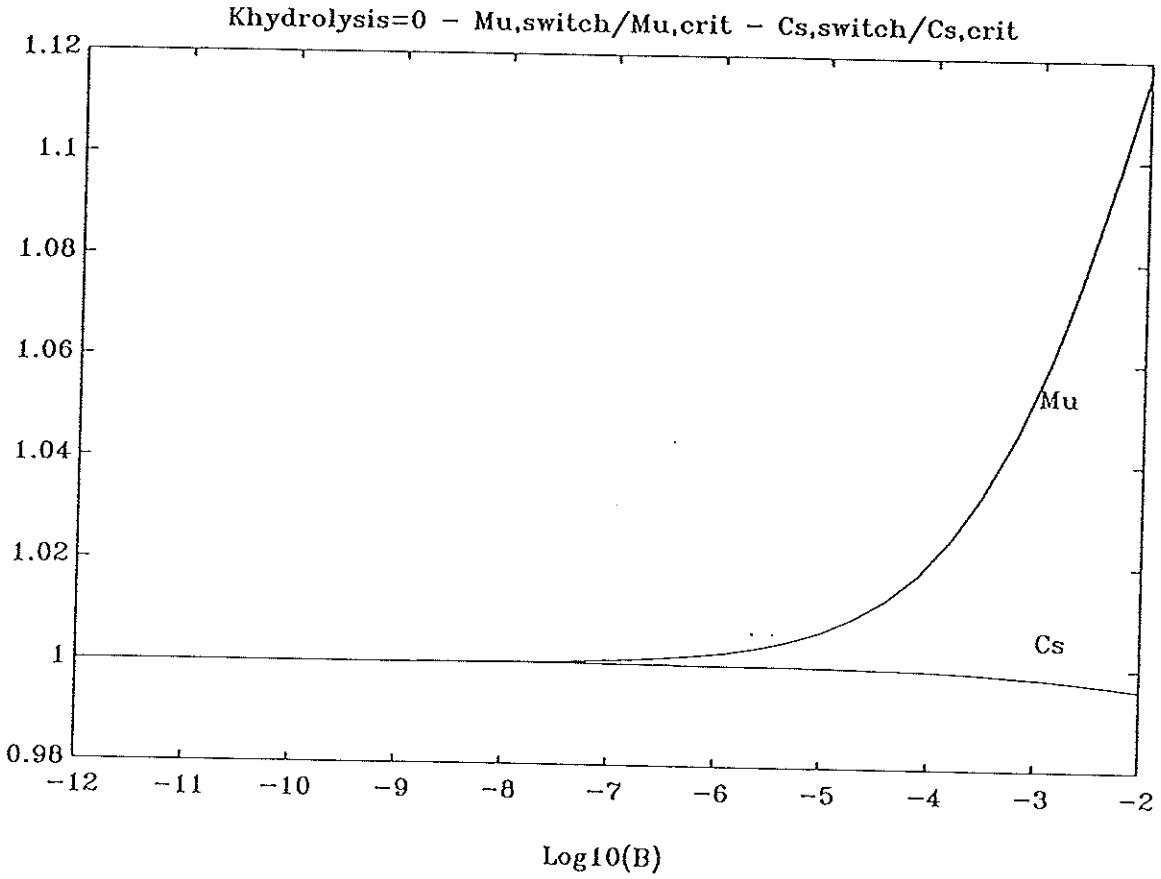

Figure 15 *Optimal switching values for μ and C_s as a function of B with $k_h = 0$*